
# CHARACTERISTICS, CAUSES, AND EVALUATION OF HELICOPTER PARTICULATE VISUAL OBSTRUCTION

THESIS

Michael P. Sullivan, Lieutenant Commander, USN

AFIT/GAE/ENY/12-S46

**DEPARTMENT OF THE AIR FORCE**
**AIR UNIVERSITY**

**AIR FORCE INSTITUTE OF TECHNOLOGY**

**Wright-Patterson Air Force Base, Ohio**

APPROVED FOR PUBLIC RELEASE; DISTRIBUTION UNLIMITED

The views expressed in this thesis are those of the author and do not reflect the official policy or position of the United States Air Force, Department of Defense, or the United States Government. This material is declared a work of the U.S. Government and is not subject to copyright protection in the United States.

AFIT/GAE/ENY/12-S46

# CHARACTERISTICS, CAUSES, AND EVALUATION OF HELICOPTER PARTICULATE VISUAL OBSTRUCTION

THESIS

Presented to the Faculty

Department of Aeronautics and Astronautics

Graduate School of Engineering and Management

Air Force Institute of Technology

Air University

Air Education and Training Command

In Partial Fulfillment of the Requirements for the

Degree of Master of Science in Aeronautical Engineering

Michael P. Sullivan, BS

Lieutenant Commander, USN

September 2012

APPROVED FOR PUBLIC RELEASE; DISTRIBUTION UNLIMITED

AFIT/GAE/ENY/12-S46

# CHARACTERISTICS, CAUSES, AND EVALUATION OF HELICOPTER PARTICULATE VISUAL OBSTRUCTION

Michael P. Sullivan, BS

Lieutenant Commander, USN

Approved:

| | |
|---|---|
| /signed/ | 17 July, 2012 |
| Dr. Donald L. Kunz (Chairman) | Date |
| /signed/ | 17 July, 2012 |
| Dr. Mark F. Reeder (Member) | Date |
| /signed/ | 17 July, 2012 |
| LtCol Ronald J. Simmons (Member) | Date |

## Abstract

A comprehensive approach to evaluation of rotorcraft brownout under degraded visual environmental conditions is presented. The results of a literature search covering the current state of brownout research are summarized. The brownout dust cloud generated by modern rotorcraft is analyzed and characterized using photographic and video data, coupled with examination of previous computer modeling techniques. A modeling analysis is performed in order to relate aircraft design and operating parameters to brownout dust cloud size is performed. The effect of vorticity in brownout dust cloud rollup is included. An augmented rating scale for pilot assessment is proposed for operational use, and the results are presented for designers and operators to approximate brownout performance of existing and future rotorcraft.

*This report is dedicated to the brave men and women of the United States Armed Forces who pilot our nations rotorcraft in harms way, in defense of our great country. I would also like to thank the staff of the Naval Aviation Center for Rotorcraft Advancement, the leadership of the USS NEW YORK, and the OPNAV N98 leadership. Finally, thanks to my wonderful wife and parents. Without the support of these people, this report would not have been possible.*

*Michael P. Sullivan*

## Acknowledgments

I would like to recognize and express my thanks to Dr. Donald L. Kunz and Dr. J. Gordon Leishman, whose support, assistance, and guidance are greatly appreciated.

Michael P. Sullivan

## Table of Contents

## List of Figures

## List of Tables

## List of Symbols

| | |
|---|---|
| $A$ | rotor disk area $\left(ft^2\right)$ |
| $a$ | exponential constant |
| $B$ | brownout parameter $\left(ft^2\right)$ |
| $\frac{B}{HR}$ | brownout parameter (*non-dimensional*) |
| $C$ | blade chord $\left(ft\right)$ |
| $C_i$ | constant of proportionality |
| $C_T$ | thrust coefficient (*non-dimensional*) |
| $C_u$ | constant of proportionality |
| $C_y$ | constant of proportionality |
| $D$ | rotor diameter $\left(ft\right)$ |
| $\overline{D}$ | mean terrain particle size $(in)$ |
| $D_e$ | duct exit diameter $\left(ft\right)$ |
| $D_W$ | water droplet size $(in)$ |
| $DL$ | rotor disk loading $\left(\frac{lb}{ft^2}\right)$ |
| $H_B$ | rotor blade height above ground (rotorcraft on ground) |

$H_C$ maximum cloud height, measured from the center of the downflow $(ft)$

$H_r$ main rotor disk plane height above ground $(ft)$

$K_g$ ground effect correction (*non-dimensional*)

$K_T$ terrain surface erosion factor (*non-dimensional*)

$\ell$ logarithmic spiral function (*non-dimensional*)

$L_{ACT}$ length of actual measurement desired $(ft)$

$L_{REF}$ length of reference feature $(ft)$

$N_R$ number of rotors (*Non-Dimensional*)

$N_B$ number of blades (*Non-Dimensional*)

$PD$ distance (measured in pixels)

$PD_{OBS}$ pixel length of desired feature in image (*pixels*)

$PD_{REF}$ length in pixels of the known reference feature (*pixels*)

$q$ dynamic pressure $\left(\frac{lb}{ft^2}\right)$

$q_F$ peak field dynamic pressure $\left(\frac{lb}{ft^2}\right)$

$q_S$ surface dynamic pressure $\left(\frac{lb}{ft^2}\right)$

$q_N$ dynamic pressure of a fully developed rotor slipstream $\left(\frac{lb}{ft^2}\right)$

$r$ radial distance from rotor center $(ft)$

| | |
|---|---|
| $R$ | rotor/blade radius $(ft)$ |
| $R_C$ | maximum cloud radius, measured from the center of the downflow $(ft)$ |
| $R_e$ | Reynolds number based on chord (*Non-Dimensional*) |
| $R_V$ | radius from the center of the downflow to the center of the vortex $(ft)$ |
| $R_X$ | radial distance ratio (*Non-Dimensional*) |
| $\frac{r}{R}$ | radial distance ratio (*Non-Dimensional*) |
| $T$ | rotor thrust $(lb)$ |
| $\frac{t}{R}$ | equivalent free jet distance (*Non-Dimensional*) |
| $\overline{U}$ | average induced velocity at rotor disk $\left(\frac{ft}{s}\right)$ |
| $u_m$ | field maximum velocity $\left(\frac{ft}{s}\right)$ |
| $\overline{U}_m$ | mean momentum velocity $\left(\frac{ft}{s}\right)$ |
| $U_N$ | induced velocity fully developed rotor slipstream $\left(\frac{ft}{s}\right)$ |
| $V$ | velocity $\left(\frac{ft}{s}\right)$ |
| $V_i$ | induced velocity $\left(\frac{ft}{s}\right)$ |
| $W$ | weight $(slug)$ |
| $X_P$ | x-axis location, referenced to lower left corner of image as (0,0) (*pixels*) |
| $X_S$ | radial distance from rotor center $(ft)$ |

| | |
|---|---|
| $Y_P$ | y-axis location, referenced to lower left corner of image as (0,0) (*pixels*) |
| $Z_V$ | height above ground of the center of the vortex $(ft)$ |
| $Z_h$ | scaling parameter for ROTWASH $(ft)$ |
| $\Gamma$ | vortex strength |
| $\Gamma_V$ | blade tip vortex strength $\left(\frac{ft^2}{s}\right)$ |
| $\Gamma_R$ | rotor wake strength $\left(\frac{ft^2}{s}\right)$ |
| $\mu$ | dynamic viscosity $\left(\frac{slug}{ft\cdot s}\right)$ |
| $\rho$ | density of air $\left(\frac{slug}{ft^3}\right)$ |
| $\rho_P$ | density of particle $\left(\frac{slug}{ft^3}\right)$ |
| $\rho_w$ | water droplet density $\left(\frac{slug}{ft^3}\right)$ |
| $\phi$ | angle (radians) |
| $\Omega$ | rotor angular velocity $\left(\frac{rad}{s}\right)$ |
| $\Omega_S$ | ground wake impingement $(HZ)$ |

## List of Acronyms

| | |
|---|---|
| AATD | (The United States Army) Aviation Applied Technology Directorate |
| ADS 33 | Aircraft Design Standard 33 |
| AFOSR | Air Force Office of Scientific Research |
| CFD | Computational Fluid Dynamics |
| DOD | Department of Defense |
| DVE | Degraded Visual Environment |
| FAA | Federal Aviation Administration |
| HQR | Handling Qualities Rating |
| LZ | Landing Zone |
| MURI | Multi-University Research Initiative |
| NASA | National Aeronautics and Space Administration |
| NAVAIR | Naval Air Systems Command |
| TRECOM | (The United States Army) Transportation Research Command |
| USAAVLABS | United Sates Army Aviation Material Laboratories |
| VCR | Visual Cue Rating |
| VTOL | Vertical Takeoff and Landing |

# CHARACTERISTICS, CAUSES, AND EVALUATION OF HELICOPTER PARTICULATE VISUAL OBSTRUCTION

## I. Introduction

### Motivation

Numerous recent operational mishaps in combat areas, including loss of aircraft, hard landings, and loss of situational awareness during degraded visual environment (DVE) operations highlight a crucial need for practical characterization of rotorcraft brownout. The current status of understanding, modeling, designing to minimize brownout, and providing operators a practical method for improving DVE operations is inadequate. This report summarizes the state of the art, and advances that state with additional data, refined analysis, and characterization of current rotorcraft.

### Background

Air accelerating downward across a thin rotor plane combined with conservation of momentum makes vertical flight possible. Using the momentum of air accelerating downward to achieve a vertical upward force is essential for helicopter flight, and also inherently creates a large air down-flow, induced velocity (Leishman, Principals of Helicopter Aerodynamics, 2006, p. 63).

It is this induced velocity:

$$V_i = \sqrt{\frac{T}{2\rho A}} \quad \textbf{(1)}$$

and resultant downwash that is one of the most distinguishing characteristics of rotorcraft, and also one of the most problematic considerations for rotorcraft flight safety in DVE situations. During normal takeoff and landing operations on prepared surfaces, this downwash creates minor hazards both to people and materials, from direct wind damage or from dust or small rocks blown around by the significant volume and velocity of the downwash. The magnitude of these hazards increases dramatically when operating from unprepared fields or hovering over the water as the induced rotor downwash interacts with loose ground and water surfaces. In these more severe environments, downwash creates clouds of particles, dust, dirt, or water, which are blown around and can greatly decrease the visibility for aircrew and damage aircraft components. The condition of rotorcraft entry into a dust cloud or water mist created by this phenomenon is known as a degraded visual environment, or more commonly, when dust is present, brownout (Figure 1).

(Swenson, 2007) Photo by Walt Harrington, Courtesy United States Air Force

**Figure 1: Brownout Example**

As the United States and other allied nations increasingly operate in desert and dusty environment, the monetary, material, and life losses caused by brownout are increasing. Brownout has been reported as a significant factor in 3 out of 4 Army helicopter mishaps in Iraq and Afghanistan and is estimated to cost the Department Of Defense (DOD) almost $100 million per year (Segall, 2012).

Despite the focus on recent losses and subsequent additional investments in research and mitigation of DVE, much of the basic understanding of the mechanisms and aerodynamics of brownout was developed in the 1950's and 1960's. This initial research used many modeling assumptions to simplify the analysis. Although many different small-scale tests were conducted, there was only one full size helicopter brownout

analysis test published in 1968. Other derivative works continued to be published through the 1970s.

After the initial research published from 1950 to 1970, the Federal Aviation Administration accomplished the next major step forward in brownout research in the 1990s. The focus of the FAA efforts was to survey and compile all research on helicopter downwash to date, and to apply the lessons learned to design civilian heliports. The culmination of these efforts, the *Rotorwash Analysis Handbook*, was completed in 1994. The handbook includes techniques for evaluating a range of effects, from penetration characteristics of rocks to flow field evaluation of the downwash clouds of tilt wing aircraft. Each of the parameters examined and developed in previous research was compiled and coded into a Fortran program. This Fortran program was contained on a floppy disk included with the hard copies of the report; however no electronic copies of the program were located.

Increased operational losses experienced during recent military operations in Afghanistan and Iraq and have pushed brownout to the forefront of concern, and it has again become a focus area for military research. Research money is being spent in an attempt to increase understanding of the mechanisms of brownout, and to reduce the effects of DVE on maintenance costs, as well as aircraft losses and the resultant loss of human life (Leishman, MURI Kick-Off Meeting "Rotorcraft Brownout: Advanced Understanding, Control, and Mitigation", 2009). Funding has been provided for research in technologies to penetrate through the degraded visual environment, for technology to display additional terrain information, for technology that further automates landings, and also for pure scientific research. Many contractors are presently developing technologies

to build synthetic vision display systems that allow the aircraft to land in DVE conditions without deterioration of the situation to dangerous levels. New initiatives in pure science include portions of the Air Force Office of Scientific Research (AFOSR) Rotorcraft Brownout Multidisciplinary University Research Initiative (MURI).

**Problem Statement**

Research, modeling, simulation, and analysis to date on rotorcraft brownout have mostly been validated with only average and peak rotorwash profile velocity data. There has been only one test completed that gathered quantitative test data on the makeup and size of the brownout cloud from an actual aircraft. This one full-scale live test was limited to a single rotorcraft and to only the configuration of that rotorcraft. Recent computational fluid dynamics (CFD) solutions have been developed and continue to be refined, but they are generally only validated to velocity profiles. Although this is helpful, it is of limited use for complete understanding of the effects of either aircraft configuration or operating parameters on DVE. Therefore, no fully validated model is available to either rotorcraft manufacturers or to the military services for including brownout parameters in design trade offs during the early stages of development of rotorcraft.

A careful analysis of available data on modern rotorcraft will be made, to include analysis of aircraft physical characteristics, as well as actual observed physical brownout parameters for the selected rotorcraft. The analysis will include examination of previous brownout work and more recent data to provide insight into the rotorcraft characteristics

that most heavily influence brownout. Relationships between these design elements and specific brownout characteristics will be examined in an attempt to determine the critical parameters that influence aspects of the brownout cloud. This analysis also aims to develop criteria that can be used to evaluate and compare the brownout performance of different rotorcraft designs.

**Research Objectives**

The objectives of this research are to evaluate the conclusions of previous research on the influence of rotorcraft design characteristics and operating conditions on brownout characteristics, as well as using new data to validate and expand upon or refute these conclusions. Additionally, a brownout parameter or parameters will be developed for use in evaluating future aircraft, systems, or tactics and to provide for future evaluation of brownout performance. The opening argument will utilize the dust cloud radius and height, and the desired end product will be a rating scale or guide for operators and designers to allow differentiation based on rotorcraft design parameters, ambient conditions, and/or landing techniques.

**Research Focus**

The focus of this research is to analyze existing and additional new data to determine whether overall vehicle weight and/or disk loading are the main influences of brownout severity, and to identify other influences that play a key role in the characteristics of the brownout cloud.

## Research Questions/Hypotheses

Previous examination has largely ignored the unsteady nature of tip vortex interaction and recirculation as potentially significant contributions to brownout severity. Although this analysis will not invalidate previous research, it is expected that unsteady aspects of the flow, not modeled by the previous analysis based on the velocity profile, will cause significant effects on the brownout characteristics of the helicopter. Recirculation may also affect the intensity of brownout in real world conditions. By using only real world data for validation, the results of this analysis will include the effects of both tip vortex interaction and recirculation, and should eliminate the attendant scaling issues.

## Methodology

This analysis will be conducted using photographs and video recordings of rotorcraft encountering brownout conditions. This media will be gathered from as many sources as possible. These photographs and videos will be carefully examined and evaluated to measure parameters of the brownout cloud for each aircraft and aircraft configuration. By gathering a wide range of media, emphasis will be placed on evaluating a broader range of aircraft with varying gross weights and disk loadings, and also with different rotor configurations. This data, recorded from the media, will be analyzed and compared to predictions from existing models, and will be compared to baseline rotorcraft physical characteristics and other related parameters.

## Assumptions

Several assumptions will be made to complete this analysis. The first assumption is that a combination of analysis data from both steady state hover and dynamic operational landing maneuvers can be used to produce an operationally significant result. The existing documentation on predicting brownout characteristics is largely aimed at a steady state hover. Operationally, helicopter maneuvers are conducted to minimize the effects of brownout. Specific evaluation of a steady state hover in DVE environments has not been conducted due to the inherent danger, so the majority of the media obtained will be from documentation of operational maneuvers. The second assumption is that all the photos and videos that are analyzed for brownout characteristics for a given moment in time are relevant, knowing that the conditions are not an ideal steady hover, but a representation of an operationally relevant maneuver. By taking a large number of media from many sources, the variation in conditions will allow an operationally relevant result. The third assumption is that dust particle size is assumed to be a baseline of less than .0197 in. as referred to in the *Evaluation of the Dust Cloud Generated Helicopter Downwash* (Rodgers, 1968, p. iii). Finally, it is assumed that rotorcraft gross weight for this analysis is a mission relevant weight, and is therefore operationally significant.

## Limitations to Scope

This research is being conducted with some limitations. All measurements for this analysis are made using photographs and video attained from various sources with varying amounts of accompanying data. Many of these media files have no information

on the weight of the aircraft or may lack specifics on the surface makeup of the landing zone. The aircraft gross weight and the dust particle size are identified as critical parameters affecting the size and intensity of the brownout cloud. However, it must be recognized that even if gross weight and particle size are known, the intensity and size of the brownout cloud are time-variant. Thus, analyzing photographs limits the utility of the photographic data to one instant in time, where it may not be known if the cloud is fully developed, or if the cloud is being affected by wind. Video analysis will provide the context for the data, but limits still apply to the availability of accompanying information. Using sound engineering judgment, emphasizing focus on the pure data, as well as more heavily weighting the data from sources that have the most accompanying specific data, will mitigate the limitations to scope.

**Implications**

When complete, the results of this research will validate, correct, and update the relationship between rotorcraft design characteristics and the characteristics of the brownout cloud the aircraft produces. A clear link between design criteria and brownout performance and characteristics will allow future rotorcraft programs to ensure that DVE performance can be taken into account along with other design requirements in the initial rotorcraft design. This could prevent consideration of brownout as an afterthought and a problem that must be solved with expensive and heavy avionics approaches. If a clear causal relationship is not found, this will indicate that the area merits further investigation.

The development of pilot and design brownout rating scales will provide a tool for developmental testers, operational testers, tactics development operators, and designers that can be used to compare the brownout characteristics of aircraft or tactics. This can be used to develop aircraft performance metrics for acquisition programs, as well as to develop the most efficient tactics to minimize brownout on rotorcraft maneuvers where brownout might be encountered. The ultimate goals are to understand brownout performance in order to improve future design and for current rotorcraft to be flown in a manner that minimizes brownout. Both of these goals lead to saving lives and aircraft.

# II. Literature Review

## Overall Historical Perspective

Some of the earliest publications relating to the study of brownout are from the National Aeronautics and Space Administration (NASA), The United States Army Transportation Research Command (TRECOM), and the United States Army Aviation Material Laboratories (USAAVLABS). This work was all published between 1959 and 1968. This early research focused on the pressure and velocity that is required to cause the ground surface to erode, the pressure patterns and velocity profiles from different rotorcraft configurations, and the amount of dust circulated and lifted by the downwash. The studies were primarily lab experiments that neglected the effects of the rotor blades and used uniform jets instead of actual rotor systems.

## Physics of Downwash Impingement

A 1959 NASA Technical Note, *D-56*, investigated the effects of downwash on the ground beneath helicopters and other vertical take of and landing (VTOL) aircraft (Kuhn, 1959). During this era, several new aircraft configurations were being developed that "range all the way from convertiplanes, which use helicopter-type rotors for hovering, to turbojet-supported types," and the increased disk loading of these configurations led to much higher downwash, for which "little quantitative information is available" (Kuhn, 1959, pp. 1,2). "The intent was to determine the manner in which the onset of disturbances varied with disk loading and height above various terrain" (Kuhn, 1959, p.

2). This study also argued that the slipstream diameter did not affect the interaction with the particles involved, and it was also to serve as a baseline for future full-scale testing.

The thrust sources examined were a 1 in. diameter nozzle, a 4 in. diameter nozzle, and a 16 in. ducted fan. The sources were directed at varying sized pans of test material including water, dirt, sod, and sand. Experiments were conducted from a variety of heights. Overall, the dust sent airborne by the downwash was compared with that of a natural dust storm, but with a reduced diameter high velocity flow region. The study showed the manner in which "the turbulent eddies … carry the dust and sand particles aloft to form the dust cloud" (Kuhn, 1959, p. 18). The overall conclusion of the NASA study is that the dynamic pressure of the outward flow is the critical parameter for lifting dust into the flow. Results for different surfaces indicated that sand and loose dirt began to erode when the maximum surface dynamic pressure is 1 to 3 $\frac{lb}{ft^2}$, wet sand and dirt erodes at 30 to 50 $\frac{lb}{ft^2}$, and water begins to spray at 1.5 to 2.5 $\frac{lb}{ft^2}$ (Kuhn, 1959, p. 1).

The height of the maximum spray and dust was recorded by motion pictures and observed to be "proportional to the square root of the surface dynamic pressure and to lie somewhere between $1.5\sqrt{q_S}$ and $2.0\sqrt{q_{S\max}}$" (Kuhn, 1959, p. 15). Additionally, inclining a lift producing device does not result in an appreciable reduction in the dust cloud for inclinations below 45 deg, which is already impractical for most applications, as a 45 deg thrust angle wastes approximately 30% of the lift (Kuhn, 1959, p. 17). Ultimately, this experiment developed some of the basics for the understanding of varied VTOL downwash, but it was conducted at a relatively small scale and was not validated

with large-scale or full-scale testing. Following this initial research, NASA dropped the VTOL downwash field and further progress was left to the Army.

One of the first Army reports on brownout was *Study of the VTOL Downwash Impingement Problem* that was completed by the Cornell Aeronautical Laboratory in 1960. This study reported on the current understanding of downwash impingement of the time, and attempted to steer both future research as well as solutions for the operational problems related to brownout. The results of NASA TN D-56 are included in this report, but the Cornell study also ties the observed phenomenon back to other pure aerodynamic flow studies, and includes more specifics on the physics of the entrainment of the particles. This report does include a detailed comparison of past experimental results to theoretical predictions, and provides some extrapolation based on this comparison. Despite the analytical work detailing the critical parameters in particle entrainment as the velocity of the flow field and the size and density of the ground particles, Cornell Labs specifically notes, "It has not been established whether or not discrete trailing vorticies can result in local velocity maximums of sufficient magnitude to have an important effect on the impingement problem"(Cornell Aeronautical Laboratory Inc., 1960, p. 18).

A significant portion of this report (26 out of 47 pages), is dedicated to future programs and research. This future programs section of the report includes several "Programs Suggested to Investigate Various Aspects of the Downwash Impingement Problem," which include recommendations for better overall understanding the problems of "avoiding entrainment," and minimizing the effects of the particles (Cornell Aeronautical Laboratory Inc., 1960, pp. 21-30). The specific recommended experiments

for future programs cover a wide array of topics and include ideas from inlet particle separators to rotor blades with air jets in the tip. The future research areas encompass nine very specific research proposals. Despite the progress made in this work, there is little recommendation to include full-scale testing of actual rotorcraft or other VTOL aircraft.

In 1960 and 1961 the US Army TRECOM commissioned 3 studies to advance the understanding of rotorcraft downwash. This research included a velocity survey and surface erosion tests (Hiller Aircraft Corp., 1961, p. 58). The three projects were summarized in a 1961 report, also published by TRECOM, which was completed by the Hiller Aircraft Corporation. The configurations evaluated include open propellers, ducted propellers, and side-by-side jets with disk loading varying from 2 to 250 $\frac{lb}{ft^2}$ and with heights varying from ¼ to 3 times the disk/duct diameter (Hiller Aircraft Corp., 1961, p. 1). Examining the results, Hiller determined that the velocity profiles for the different downwash sources configurations are very similar. After examining the data from varying the height and loading of several thrust configurations, Hiller determined that the onset of erosion is initiated by the maximum field dynamic pressure exceeding the critical pressure for the surface. The maximum field dynamic pressure itself is related to the disk loading and height of the thrust device. Hiller also evaluated inclining the thrust vector, and determined there was little reduction in dynamic pressure at the point of ground interaction. Overall, the results from this report correlated well with the previous NASA study.

The overall primary observations of this review are that "the surface critical dynamic pressure [of the surface] and the field maximum dynamic pressure $q_{FM}\left[q_F\right]$, determine if erosion will be encountered," and "the field maximum pressure varies directly with disk loading and inversely but in a non-linear fashion with $\frac{Z}{D}\left[\frac{h}{D}\right]$" (Hiller Aircraft Corp., 1961, p. 2).

Based on the observed relationships, this study concludes "the most direct method of reducing field dynamic pressure…is to reduce the disk loading" (Hiller Aircraft Corp., 1961, p. 10). Additionally, increasing the height of the downwash source will also decrease the field dynamic pressure, although "if the design $\frac{Z}{D}\left[\frac{h}{D}\right]$ is > 0 the reduction in the maximum dynamic pressure …are insignificant" (Hiller Aircraft Corp., 1961, p. 10). This report is the first quantitative link between disk loading and the intensity of brownout, but it also links the height of the rotor as another significant cause.

Cornell Aeronautical Laboratory conducted another study, published in 1963, *Theoretical and Experimental Studies of Impinging Uniform Jets*. This study examines a uniform jet, 12 inches in diameter, to isolate the aerodynamic characteristics of the downwash field from effects of individual blades of a rotor system. Extensive sampling of parameters along the surface upon which the downwash impinges allowed Cornell to merge theory with empirical data.

Three distinct areas of the downwash outflow are examined; the laminar boundary layer in the vicinity of the stagnation point (the center of the downwash for a stationary rotor), the wall jet, or turbulent boundary area, and the transition area between the two.

The diameter of the laminar boundary layer and the transition area are based on the Reynolds number of the nozzle. Figure 2 displays this relationship.

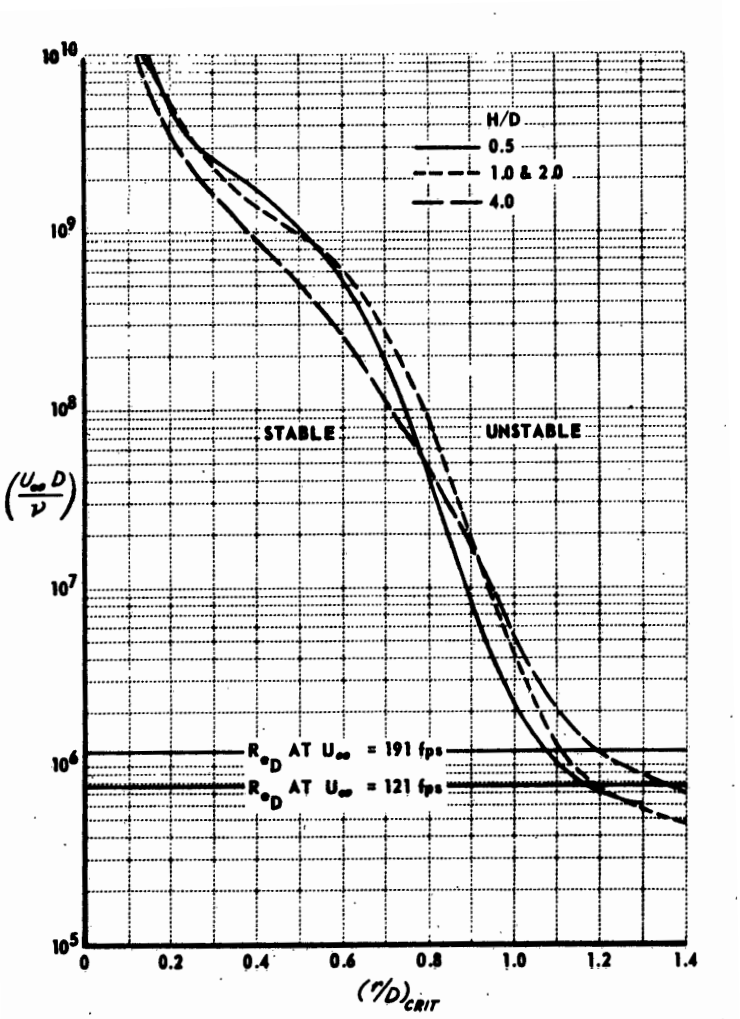


(Cornell Aeronautical Laboratory Inc., 1963, p. 86)

**Figure 2: Location of Boundary Layer Transition**

The transition area begins at the point where the laminar flow becomes unstable. After a short period of transition, the wall jet area begins. The velocity in the wall jet area is

related to the non-dimensional radius (radius of location non-dimensionalized by rotor radius):

$$\frac{u_m}{\overline{U}} = C_1\left(\frac{r}{R}\right)^a \qquad \textbf{(2)}$$

where data reduction determines the constant of proportionality and the exponent to be $C_1 = 0.46$ and $a = 0.933$ (Cornell Aeronautical Laboratory Inc., 1963, pp. 19,21). An example radius vs. velocity profile including all three regions is found in Figure 3.

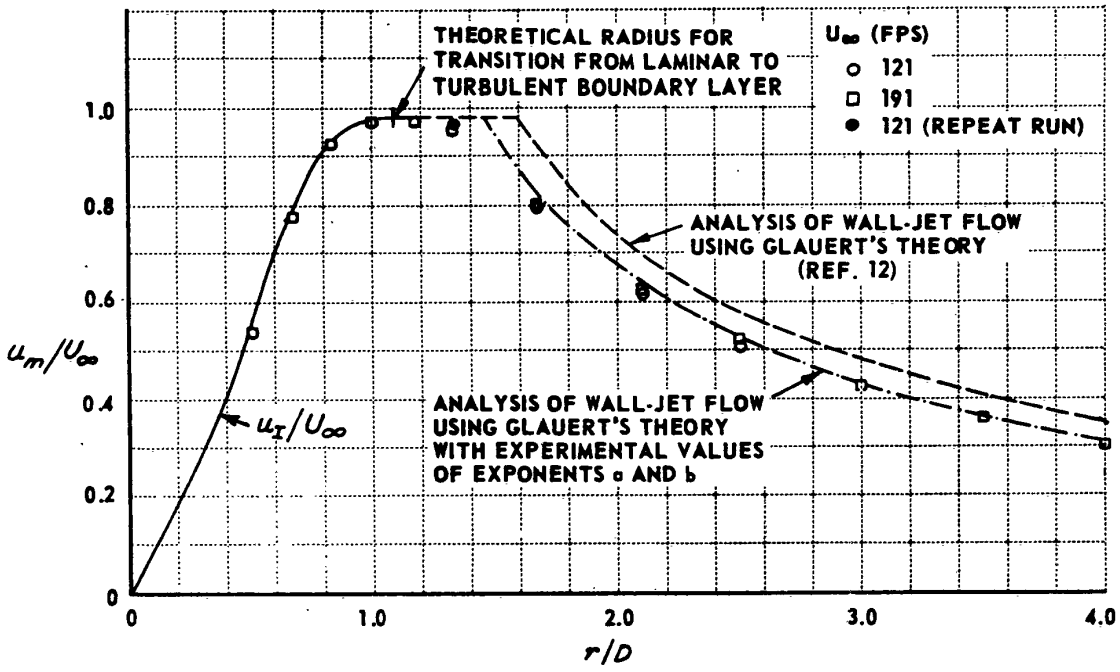


(Cornell Aeronautical Laboratory Inc., 1963, p. 89)

**Figure 3: Experimental Maximum Local Velocity Profile**

Overall, the analysis of the velocity profiles in the boundary layer "resulted in good to excellent agreement with experimental data" (Cornell Aeronautical Laboratory Inc., 1963, p. 3). This validation of theory creates a solid baseline for future research.

**Synthesis**

TRECOM published an additional comprehensive study utilizing all previous research, over 38 individual reports in 1964, with the focus of determining specific design characteristics and their effects on the downwash and the results of its impingement. "The objective of this program was to utilize existing data for the preparation of design charts for VTOL aircraft to aid in the establishment of aircraft designs that will alleviate the operational conditions resulting from downwash impingement on terrain" (DYNASCIENCES Corporation, 1964, p. 1).

This analysis affirms that aircraft parameters which affect the dynamic pressure of rotor downwash are primarily disk loading, rotor plane height above the ground, and number and configuration of lift devices. There are two critical regions, the laminar boundary layer, approximately $\frac{x_s}{d_e} < 2.0$ and wall jet region, where $\frac{x_s}{d_e} > 2.0$. "Within the circular area bounded by $\frac{x_s}{d_e} < 2.0$, the surface dynamic pressure and the static pressure on the ground, both primary causes of surface erosion, are significantly dependent upon disk loading and nozzle height" (DYNASCIENCES Corporation, 1964, p. 9). In the region outside two rotor diameters from the center of the downwash, the effect of the rotor height above the ground on the outflow characteristics rapidly diminishes, while the disk loading increases. The maximum surface dynamic pressure is related to the radial distance ratio and average dynamic pressure at the jet/rotor exit:

$$\left[\frac{(q_s)_{\max}}{q_N}\right]\left[\frac{x_s}{d_e}\right]^2 = 1.4 \qquad \left\{\frac{x_s}{d_e} > 2.0 \right. \qquad \textbf{(3)}$$

This relationship matches well within the region of a sample set of experimental data presented in Figure 4. Inside of two radii, the theory does not consistently produce

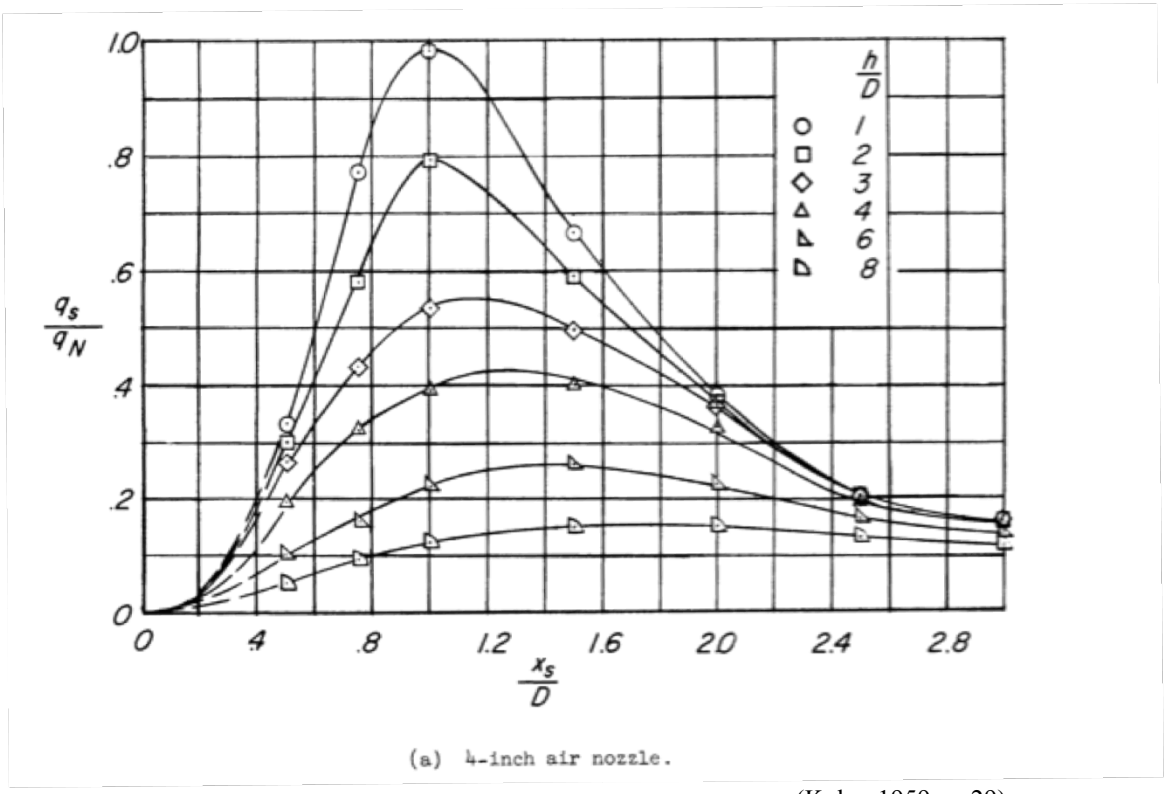


(Kuhn, 1959, p. 29)

**Figure 4: Maximum Surface Peak Dynamic Pressure**

accurate predictions of the maximum pressure observed. The most accurate method conceived to determine the maximum field pressure $q_F$, or $\frac{q_F}{q_N}$ in Figure 4, is "by utilizing the decay data of a jet discharging into free air…for a direct correlation of $q_F$" (DYNASCIENCES Corporation, 1964, p. 10). The decay of a jet can be seen in Figure 5. Calculating the actual location of $q_F$ is more difficult and "final results have not been obtained" from "a more recent iterative method" (DYNASCIENCES Corporation, 1964, p. 10).

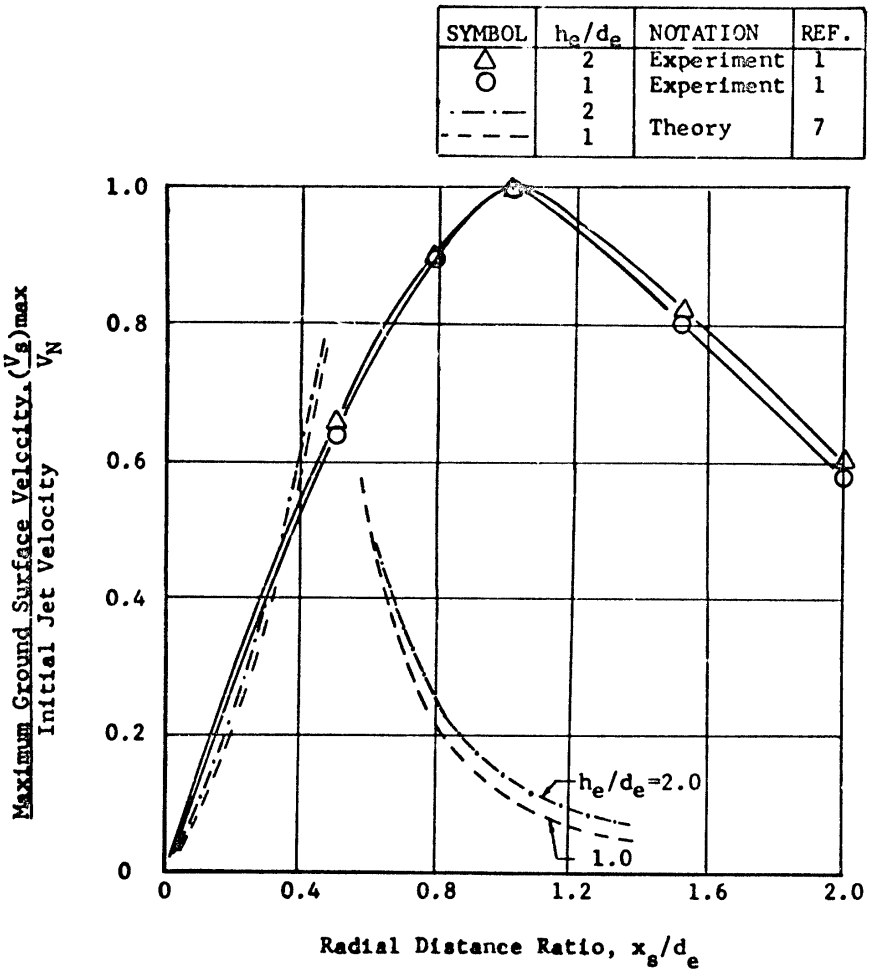


(DYNASCIENCES Corporation, 1964, p. 60)

**Figure 5: Theoretical vs. Experimental Velocity Distribution**

This TRECOM/DYNASCIENCES review also contains a significant explanation of dual lift devices. The primary difference between single and dual lift rotorcraft, as determined by the study is that the presence of two lift devices causes a slight increase in dynamic pressure along the symmetric axis with an associated increase in radial outflow.

The study concludes that there are four basic options to reduce the effects of the dust cloud caused by downwash impingement on a surface; 1) structures placed to

disperse the flow, 2) coating the ground with a gel or other binder, 3) capturing the dust particles, or 4) reducing the downwash velocity. Although the report re-affirms that basic first order relationships are observed, it has many recommendations for further studies that could increase the accuracy of the predictions. However, few of these proposed research areas were ever followed with additional experiments.

The above information from the 1964 TRECOM report is collated and re-stated data from previous reports. The primary advances made during this study are from careful building of "methods and design charts for estimating the operational conditions arising from operations of VTOL aircraft in the proximity of the ground" (DYNASCIENCES Corporation, 1964, p. 5). The parameters used for these calculations include the dynamic pressure of the jet, the height above terrain, and jet diameter, and the results of the calculations include data such as dust cloud radius and dust cloud height. Other parameters are included in the report, but are not within the scope of this investigation. The calculations relating to dust cloud characteristics will be detailed in review of additional literature and in the Methodology section of this Report.

**Flight Test**

Several years after the TRECOM/DYNACIENCES design study was completed in 1964, a full size flight test was performed. This 1968 study, by MSA Research Corporation, is one of a few full-scale flight tests that have been performed with the primary purpose to quantitatively evaluate the dust cloud of a helicopter (although other full size tests have been conducted to collect velocity profiles or similar data over water).

This report references two earlier related full size tests conducted by Kaman Helicopters and the Boeing company, but neither report was able to be obtained for direct review.

This particular 1968 test was originally conceived to be comprehensive, including a single rotor helicopter in addition to a tandem rotor in 5 locations at three loadings for each condition. However, due to monetary and other restrictions, it was ultimately severely limited in scope to using only one rotorcraft, three locations, and only a 15% variation in disk loading. The test was conducted utilizing a tandem-rotor H-21 and data was gathered at three landing zones around the country, with each landing zone having different ground composition. One of the key conclusions from this flight test is that even during successive tests under identical test conditions, the dust concentrations changed by about 15% from one test run to the next, so even in near identical conditions, the dust cloud composition varies greatly (Rodgers, 1968, p. 4).

The primary data from this report consists of tables of the weight and size of the particles recovered at each sample station. These tables are collated into several visualizations, and an example can be found in Figure 6. With the tandem-rotor configuration, the dust concentrations were highest at the rotor blade overlap, and lowest beneath the rotor hubs, near the stagnation point of the downwash.

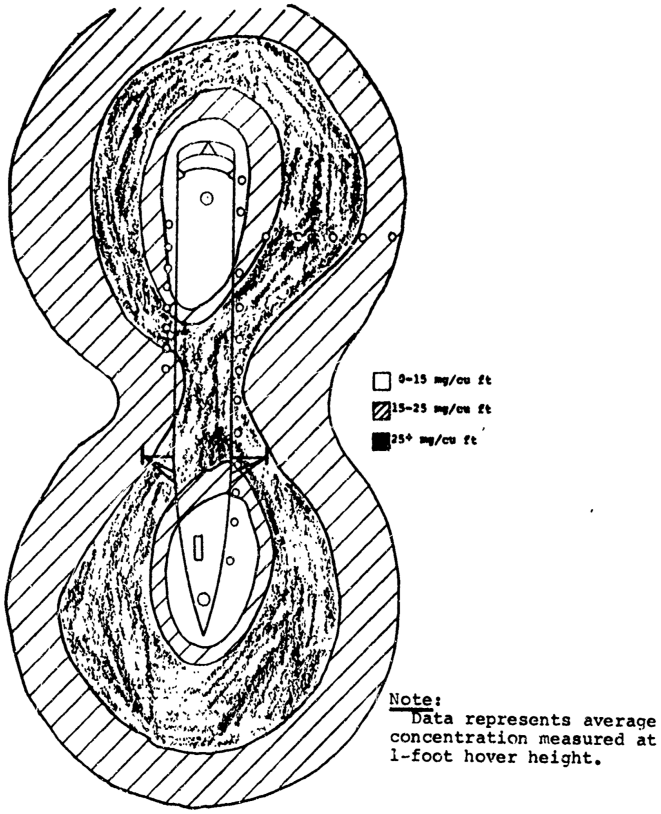


(Rodgers, 1968, p. 18)

**Figure 6: Flight Test Dust Distribution Diagram**

Another key observation during this test is that all the dust sampled was less than 500 μm (Rodgers, 1968, p. iii). Also, attempts to include pilot visibility in this study using both a radiometer to measure light and ground targets for the pilots to observe were largely inconsistent and were not repeatable. Despite the positive steps made in understanding the dust cloud by this study, its limitation to the single rotorcraft, 3 test sites, and 15% disk loading variation limit the number of conclusions that can be made.

**Comprehensive Analysis**

In 1985, the Federal Aviation Administration initiated a program "to develop a rotorwash analysis methodology… to better understand, mathematically model, predict with analysis, and develop techniques and design guidance for avoidance of many of the more important types of rotorwash-related mishaps" (Ferguson, Rotorwash Analysis Handbook, Volume I: Development and Analysis, 1994, p. 1). This program consisted of a 9 year project that reviewed 78 previous reports, developed several iterations of computer code, incorporated data from concurrent DOD full-scale tests, and consolidated test data from all previous tests. The result of this ambitious project is the FAA's *Rotorwash Analysis Handbook*. The Handbook consists of two paper volumes and a collection of Fortran files (known collectively as ROTWASH). It was published in 1994 and is a broad examination of "virtually all work done on this issue by various U.S. government agencies" (Ferguson, Rotorwash Analysis Handbook, Volume I: Development and Analysis, 1994, p. i). This report consists of three sections that include "analytical mathematical models that have been developed to investigate rotorcraft downwash flow fields as well as correlation with flight and model test data," "development of a hazard analysis methodology and to mathematical modeling and analysis of many of the more common types of rotorwash-related hazards," and documentation of the ROTWASH Fortran code (Ferguson, Rotorwash Analysis Handbook, Volume I: Development and Analysis, 1994, pp. 2-3). It also includes several appendices that include additional model/flight test correlation data, "a comprehensive bibliography of rotorwash-related documents" (Ferguson, Rotorwash Analysis

Handbook, Volume I: Development and Analysis, 1994, p. 3), and the Fortran ROTWASH code.

The analysis section of the FAA report is itself divided into several sections to detail the flow field of the rotor downwash. The first analysis section is a detailed step-through of the analytical method for analyzing the wall jet outflow, as defined earlier. Also included are modifications to the baseline analysis to allow tilted rotors as well as multi-rotor systems to be analyzed. The second section focuses on the ground vortex, which occurs primarily when there are ambient winds or during air-taxi. The existence of the flowfield wrap-up into a ground vortex is well known. However, "until further experimental data are obtained …results from this mathematical model must be presumed suspect" (Ferguson, Rotorwash Analysis Handbook, Volume I: Development and Analysis, 1994, p. 57). The remaining analysis mirrors fixed wing tip and trailing edge vortex theory for rotorcraft in situations where the ground vortex has been blown underneath the rotorcraft. The wall jet and forward flight methods of analysis are "validated extensively" (Ferguson, Rotorwash Analysis Handbook, Volume I: Development and Analysis, 1994, p. 5) with results from full-scale testing of CH-53, XV-15, MV-22, CL-82, and an SH-60B. An example of the collected data can be found in Figure 7.

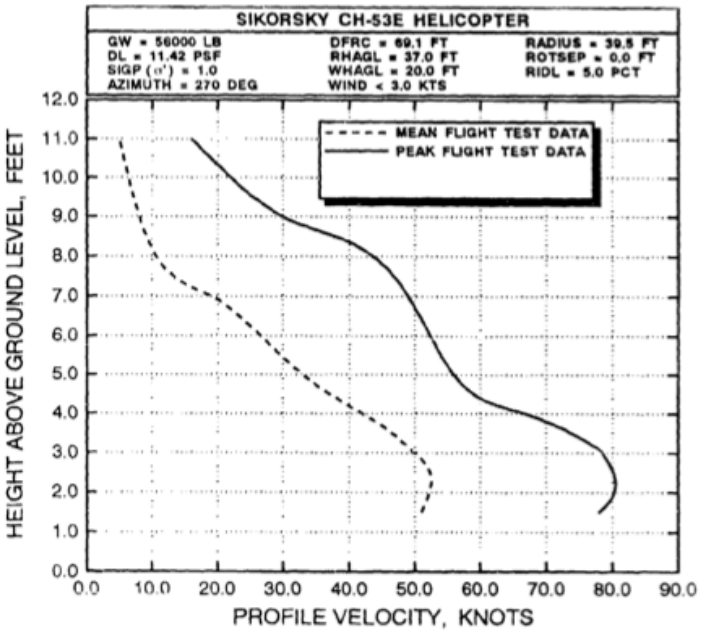


(Ferguson, Rotorwash Analysis Handbook, Volume I: Development and Analysis, 1994, p. 18)

**Figure 7: Example Velocity Profile Data**

Each of the full-scale tests collected somewhat different data and the wall jet model was successfully validated. However, the limited vortex experimental data prevented a thorough validation of the vortex theory.

The second major analysis section of the FAA report examines the hazards created by the downwash field defined and determined in the first major section. Some of the rotorwash hazards analyzed in this section include effects on other rotorcraft, on fixed-wing aircraft, on structures, on ground vehicles, and the dangers of entrained debris and particulate clouds. The rotor cloud portion of the analysis is based primarily on the maximum surface dynamic pressure and the terrain surface erosion factor. In addition to the pure velocity/pressure component, the rollup of the outflow into a vortex is taken into consideration utilizing vortex theory. A representation of the vortex location and the resulting dust cloud from this section can be found in Figure 8.

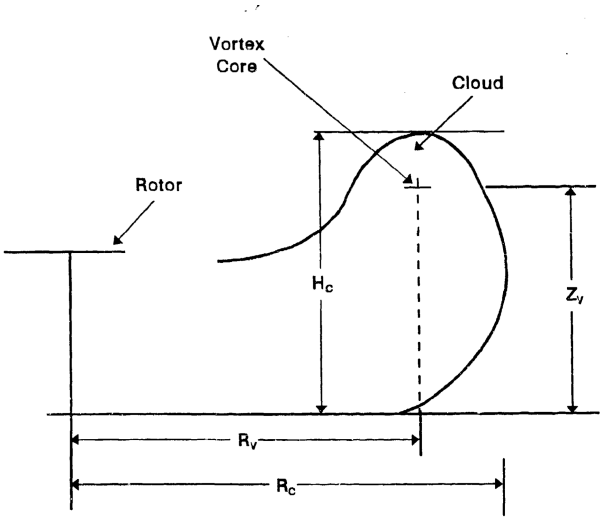


(Ferguson, Rotorwash Analysis Handbook, Volume I: Development and Analysis, 1994, p. 260)

**Figure 8: Representation of Particulate Cloud Geometry**

Using the notation of Figure 8, the location of the vortex rollup can be calculated utilizing equations 4 and 5, which results in a predicted dust cloud of the height and radius calculated by equations 6 and 7 (Ferguson, Rotorwash Analysis Handbook, Volume I: Development and Analysis, 1994, pp. 261,264):

$$R_V = 0.785 R_C \tag{4}$$

$$Z_V = 0.329 R_C \tag{5}$$

$$R_C = R\left(\frac{\sqrt{K_T}}{C_3 \frac{1}{2}\rho_A \overline{U}_m^2 C_u^2}\right)^{-0.437} \tag{6}$$

$$H_C = \ell_V + Z_V \tag{7}$$

In addition to the dust cloud analysis, this section also includes detailed analysis of other rotorwash hazards.

The remaining major FAA report segment, which documents the methodology for applying the aforementioned theory, is split between Volumes I and II of the handbook.

The methodology in Volume I includes a scenario that is "designed to be instructional guides for anyone using the methodologies and data in this report" (Ferguson, 1994, p. 281). The methodology used in the scenario is also the basis for the Fortran code, ROTWASH. Several sections in Volume II provide the text of the Fortran ROTWASH code as well as the user guide "designed to guide the reader through a step-by-step explanation on the use of each program software option" (Ferguson, 1994, pp. D-1

Despite comprehensive, in-depth research and analysis collected in this document, the resulting model was only thoroughly validated with respect to velocity profile information. This limits its utility for other parameters. For example, based on limited particulate and water cloud testing, for the dust cloud prediction it is "risky to claim that the model is good for anything other than general estimation purposes...[and] appears to be somewhat overpredictive of the cloud height" (Ferguson, 1994, p. 270). Also, in the dust cloud analysis, the ROTWASH program does not account for any ambient wind, the interaction of which with the rotorwash has not been thoroughly studied. The report calls out two areas for future research, including experiments to increase the database available for flowfields during different wind conditions, and "for validation of wind tunnel testing methods" (Ferguson, 1994, p. 318).

**Recent and Ongoing Research**

Several papers were presented at conferences in 2009 that investigate, using CFD or other models, methods to simulate or predict the brownout characteristics models of rotorcraft. This recent work is based on various methods of improving previous analysis

by carrying the vortex structures and energy through the interaction with the ground and dust. Vortex confinement is being examined by Stanford University to improve the prediction of vortex interaction in complex scenarios with promising results when referenced visually to previous vortex visual testing (Hahn & Iaccarino, p. 1). The University of Glasgow has conducted a detailed computational fluid dynamics approach to analyzing the particle/air system, but again, this model is only validated with visual analysis of several approach, hover, and takeoff scenarios (Phillips & Brown, 2009, pp. 1416, 1428).

The most completely analyzed solution is the free wake model included in the Comprehensive Hierarchical Aeromechanics Rotorcraft Model (CHARM) program developed by Continuum Dynamics, Inc (Wachpress, Whitehouse, Keller, McClure, Gilmore, & Dorsett, 2009, p. 10). This model was validated with the same CH-53 and XV-15 average and peak outwash velocities used to validate the FAA ROTWASH program. Additional modeling designed to replicate the visual aspects of brownout for simulators appears to visually match well with expected brownout characteristics and correlates well with the 1968 Rodgers full-scale dust collection test, resulting in a solution that is "more accurate than any other currently published brownout analysis predictions" (Wachpress, Whitehouse, Keller, McClure, Gilmore, & Dorsett, 2009, p. 18).

**Current Multi University Research Initiative Efforts**

The Air Force Office of Scientific Research (AFOSR) awarded a MURI focused on understanding and mitigating brownout in August 2008. There are 12 individual tasks in this initiative spread across subjects from rotor and fuselage aerodynamics to the wake vortices/ground interaction. It is being performed by the University of Maryland, Arizona State University, Iowa State University, and Dartmouth College, and is scheduled to span several years. Several of the tasks have progressed through initial tests and some results are published. Upon completion of all aspects of the research, a more precise, accurate, and comprehensive analysis tool, called ABATE, is expected to be developed. This simulation tool will be composed of modules that have been developed and validated by different portions of the MURI, which as a whole will provide an ability to simulate to a much higher level of fidelity and accuracy than any previous rotorwash analysis tools.

# III. Methodology

## Data Acquisition

The primary data in this examination consists of rotorcraft configuration information, as well as rotorcraft cloud parameter information. All physical configuration data is collected from various open source data, including the FAA's Rotorwash Handbook Volume II. A data call was put out through Naval Air Systems Command (NAVAIR) and Army Aviation Applied Technology Directorate (AATD) for media of testing in dusty environments. The cloud parameter information is measured from digital photographs and digital video. The photographs and video received are from a combination of flight test footage, documentation of military operations, and public affairs video, and were acquired from a variety of sources including individuals, the Internet, and academic meeting presentations, as well as from NAVAIR and AATD programs of record.

The overall reference axis used for analyzing the dust clouds is the aircraft fixed body axis. This is a Right Hand, Orthogonal axis system with the origin at the center of gravity of the aircraft, the x-axis directly out the nose of the aircraft, and the z-axis directly down from the origin relative to the aircraft while sitting on the ground (assumed to be a plane) as seen in Figure 9.

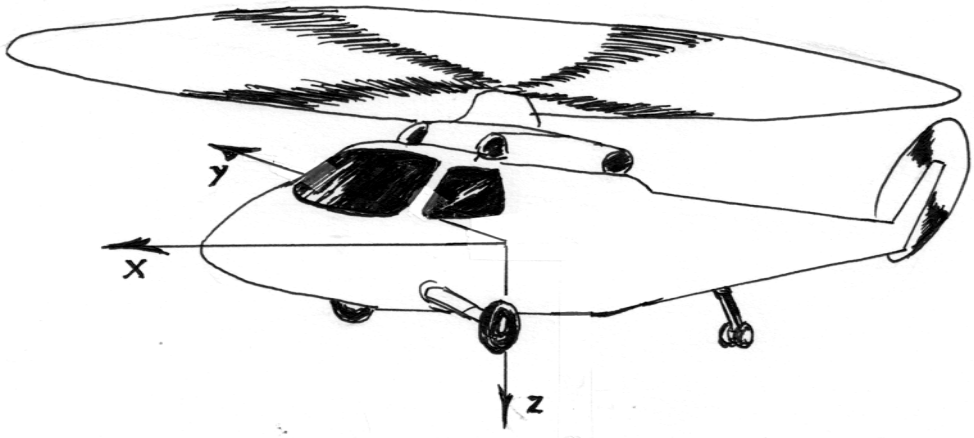


**Figure 9: Aircraft Fixed Body Axis**

For rotorcraft with multiple lifting rotors, the analysis includes a defined *interaction plane,* the plane along which the flows from the separate rotors meet and affect each other. A representative orthogonal vector, referenced from the plane between the two rotor hubs and perpendicular to the ground, as seen in Figure 10, will be

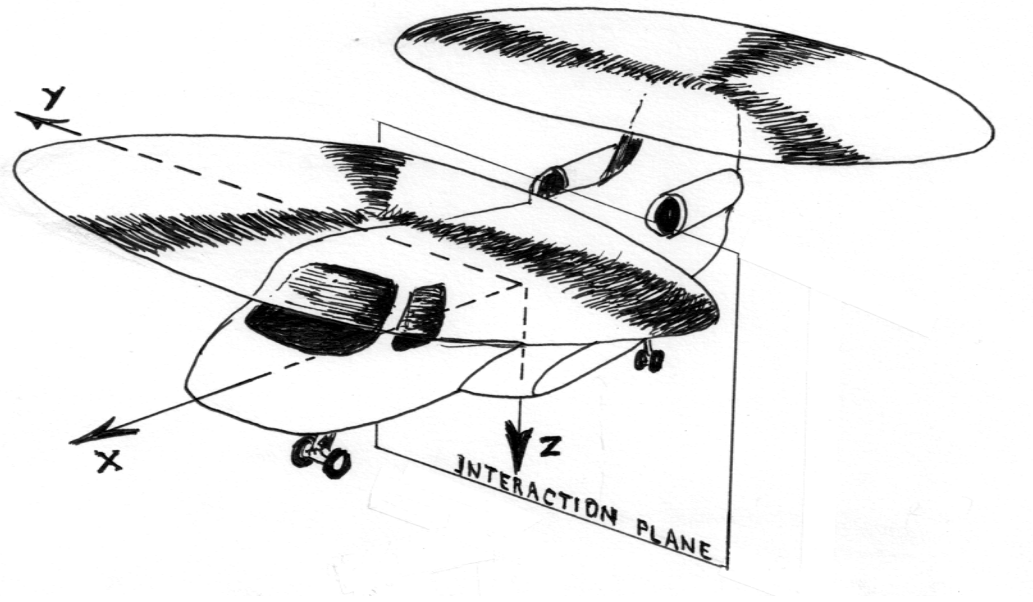


**Figure 10: Interaction Plane**

coincident with the y-axis for a side by side rotor configuration, and coincident with the x-axis for a tandem rotor configuration.

Each media file was examined to determine specific, relevant dimensions that could be clearly measured, based on the specific visible cloud characteristics. For each cloud parameter to be measured, a visible aircraft feature, to be measured along the same orthogonal axis as the desired cloud measurement, was identified. Examples of these reference features are; a rotor perpendicular to the helicopter body, distance between landing gear, and distance from landing gear to rotor hub. The known dimensions of the aircraft features (generally available from the data sources above) provide accurate benchmarks for faithfully measuring cloud parameters.

In this investigation, specific standards are used in the cloud parameter measurements. Dust cloud height measurements are made to the lowest height of the cloud that is continuous for the entire length of the aircraft, and referenced to the ground beneath the rotorcraft. The inner and outer radii of the dust cloud are measured from the center of the rotor hub. For the inner cloud radius, the minimum distance from the center of the rotor to the observed dust cloud is recorded. For the outer radius, the maximum radius of the cloud in the forward hemisphere of the aircraft is used. For a multi-rotor helicopter, the radius measurements are taken from the nearest rotor hub in the observed location where the additional rotor influence would be minimized. For multi-rotor helicopters, additional measurements are made along the rotor interaction plane. Cloud measurements on the rotor interaction axis are made at the smallest and largest radii observed along the axis. Throughout the measurements, small errors due to distortion

from perspective are neglected, since the known corresponding aircraft reference measurements suffer equivalent distortion and the comparison is still valid due to the proximity of both dimensions. Additional distortion caused by diminishing perspective is also neglected, since the depth of the measurements of interest is much smaller than the distance the photos are taken from in nearly every case. Time information is measured using a stopwatch to the nearest 1/10 of a second.

Once each desired cloud measurement is identified, the x and y coordinates of the starting and ending pixels of the measurement are recorded. The x and y coordinates for the known reference distance along the same orthogonal axis as the measurement are also recorded. From the coordinates, the pixel distance is calculated:

$$\left(\left|X_{P2} - X_{P1}\right|\right)^2 + \left(\left|Y_{P2} - Y_{P1}\right|\right)^2 = PD^2 \quad \textbf{(8)}$$

The ratio of the pixel distance of the reference item to the actual length is used to determine the length of the cloud parameter being measured:

$$\frac{PD_{REF}}{L_{REF}} = \frac{PD_{OBS}}{L_{ACT}} \quad \textbf{(9)}$$

An example of a photo with the analyzed measurements in included in Figure 11. The sample is a V-22 in a hover. The vertical reference measurement is the length of the engine nacelle and the length reference measurement is the overall length of the fuselage.

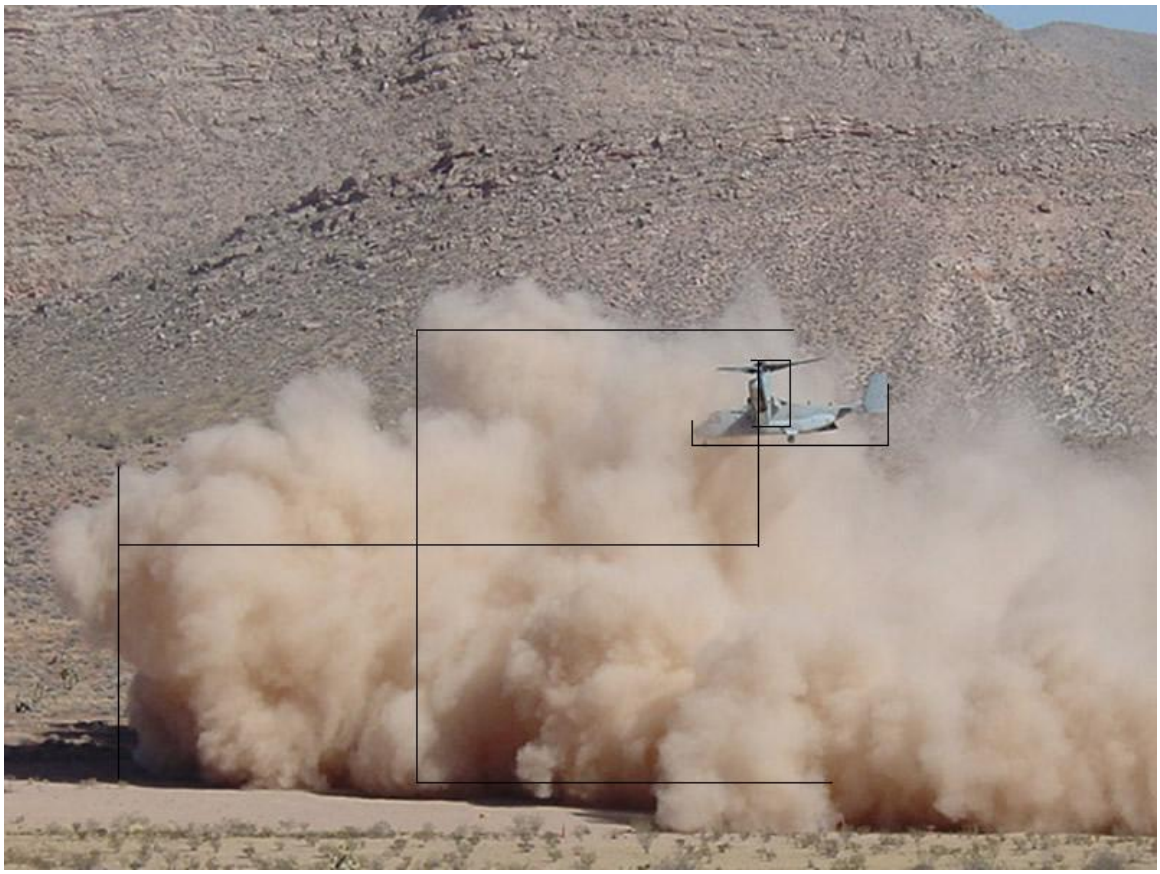

(Awaiting AFRL verification of permission) Photo by Walt Harrington, Courtesy United States Air Force

**Figure 11: Sample Photograph With Reference Distances Indicated**

Data from many aspects of the rotorcraft configuration is required for the various aspects of the analysis. This configuration data is primarily sourced from the "Rotorwash Analysis Handbook, Volume II" (Ferguson, 1994, pp. A-2 - A-6) and is suplimented by *Jane's All the Worlds Aircraft*, 2009. A selection of this compiled configuration data, including rotor configuration, gross weight, rotor dimension, and rotor speed information, is summarized in Table 1. The actual in-flight gross weight for each aircraft can vary greatly between the rated maximum gross weight and the empty weight. For consistency in analysis, a *mission representative* weight was developed. The total useful load is calculated by subtracting the base weight (including no engine oil, fuel, crew, or mission

gear) from the maximum gross takeoff weight. A mission representative load for each aircraft is calculated as 2/3 of the total useful load (total weight of engine oil, fuel, aircrew, and payload). The mission representative load is then added to the aircraft base weight to calculate the mission representative weight. This mission representative weight is included in Table 1.

**Table 1: Aircraft Information**

| Rotorcraft | Rotor Configuration | Mission Representative Gross Weight (*lbs*) | Rotor Diameter (*ft*) | Rotor Speed (*rpm*) |
|---|---|---|---|---|
| UH-1N | Single Main | 8,866.7 | 48.0 | 324 |
| Lynx | Single Main | 9,727.7 | 42.0 | 305 |
| Tiger | Single Main | 11,794 | 42.7 | 315 |
| AH-64A | Single Main | 18,333 | 48.0 | 289 |
| UH-60L | Single Main | 18,600 | 53.7 | 258 |
| UH-3 Mk3 | Single Main | 18,667 | 62.0 | 203 |
| CH-46D | Tandem | 19,333 | 51.0 | 264 |
| Mi-17 | Single Main | 24,386 | 69.9 | 305 |
| EH-101 | Single Main | 28,330 | 61.0 | 210 |
| CH-53D | Single Main | 36,833 | 72.2 | 185 |
| CH-47 | Tandem | 41,667 | 60.0 | 225 |
| V-22 | Side-by-Side | 46,220 | 38.0 | 397 |
| MH-53E | Single Main | 60,075 | 79.0 | 185 |

(Ferguson, 1994) (Jackson, 2009)

**Data Correction and Error Bounding**

Air density is required for the calculations in order to predict the dust cloud and to perform some of the rotorcraft parameter calculations. Although the specific locations for the majority of the media are not recorded, based on the sources of the media, and on the visible terrain features, much of the media is from the Yuma Proving Ground, the deserts of western and southern Iraq, and from central and southern Afghanistan.

Individual media file air density analysis is not possible due to the limited information on location and ambient conditions. Although detailed density analysis would increase the fidelity of the calculations of the parameters, there is simply not a sufficient data base of ambient conditions to support individual calculations. Variation of density as a source of error, however, is bounded by examining the high and low densities that may be encountered.

The altitude of the Yuma proving ground airfield is 324 *ft msl* where normal temperatures reach 45° *F* in the winter and 107° *F* in the summer (Weather Underground, 2011). Iraq and Afghanistan have more extreme altitudes and average temperatures, which vary from sea level to almost 25,000 *ft msl* (Central Intelligence Agency, 2011). Although it is possible to conduct rotorcraft landing and takeoff operations above 10,000 *ft* pressure altitude, due to operation limitations for US Rotorcraft and the type of operations conducted above these altitudes, an outside observer would not likely have access to take photographs at these locations, and so it is highly likely that all media is from altitudes of less than 10,000 *ft*.

Examining the lowest density that might be represented in the selected media, 1972 Air Force study indicates that even during extreme weather conditions, high temperatures and humidity will not decrease density more than 12% less than the Standard Day Atmosphere (Cormier, 1972, p. 8). The Standard Day Atmosphere at 10,000 *ft* has a density of $1.755 \times 10^{-3} \ \frac{slug}{ft^3}$, with a 12% reduction giving the lowest density of $1.545 \times 10^{-3} \ \frac{slug}{ft^3}$, which is equivalent to a density altitude of approximately 14,000 *ft* (McCue, 1994, pp. AII-3).

Examining the highest density that might be represented, a *Synopsis of Background Material for MIL-STD-210B, Climatic Extremes for Military Equipment* identifies the maximum high density for operations as $3.337 \times 10^{-3} \frac{slug}{ft^3}$ (Sissenwine, 1974, p. 114). This value is based on the lowest temperatures observed on earth of -78°*F* and pressure of 1050 *mb*. However, the highest density that is likely to be observed in these photos would be at sea level in Iraq, with extreme lows near 25°*F* (Franklin, 2009). At -1,000 *ft* pressure altitude and 25°*F*, results in a likely minimum density altitude of -2,000 *ft* can be calculated with a density altitude chart (McCue, 1994, pp. AII-3).

A relevant, representative median density is calculated based on the discussion of bounding the environmental conditions. A reasonable density altitude range of -2,000 *ft* to 14,000 *ft*, gives an operationally relevant median density altitude of 6,000 *ft*. The median density altitude of 6,000 ft gives a density of $1.987 \times 10^{-3} \frac{slug}{ft^3}$, which is used as the base density for the analysis. This is the only density used for subsequent analysis, but a sensitivity analysis using several other densities shows that for an H-60, even though the predicted downwash velocities and the maximum dynamic pressures vary, as seen in Table 2, the predicted dust parameters do not vary by density.

**Table 2: Results of Density Variation**

| Reference Density | Density ($slug/ft^3$) | Fully Developed Induced Velocity (ft/s) | Dust Radius (ft) | Dust Height (ft) |
|---|---|---|---|---|
| Base Density | $1.987 \times 10^{-3}$ | 90.98 | 234.4 | 110 .1 |
| Standard Sea Level | $2.378 \times 10^{-3}$ | 83.16 | 234.4 | 110 .1 |
| Maximum Density | $3.337 \times 10^{-3}$ | 70.20 | 234.4 | 110 .1 |
| Minimum Density | $1.545 \times 10^{-3}$ | 103.17 | 234.4 | 110 .1 |

## Data Processing

All measured and recorded reference data is collated in spreadsheets, where initial basic measurement processing is completed, as well as unit any required initial unit conversion. All literature reviewed, as well as the FAA rotorwash prediction program, are all developed using English units. Due to this legacy, SI units are limited to a couple of dimensions gathered for European and Russian aircraft. For consistency, all SI or other dimensions requiring conversion are converted to English units in accordance with the conversion factors listed in Table 3. After conversion, the numbers are reduced to the same significant figures as the source document, with numbers ending in the numeral five and higher rounded up. Upon completion of initial conversion and calculations, the data from the spreadsheets is imported into MATLAB for calculation of the predicted outcome.

**Table 3: Conversion Factors**

| Metric Unit | English Unit |
|---|---|
| 1 meter | 3.2808 feet |
| 1 micrometer | $3.9370 \times 10^{-5}$ inches |
| 1 kilogram | 0.068521 slugs |
| 1° Celsius | $\frac{5}{9}\left(^{\circ}Fahrenheit - 32\right)$ |
| 1 Millibar | $2.9530 \times 10^{-2}$ inches of mercury |

**Dust Cloud Predictions – Data Utilization and Computer Program Functionality**

Each media file successfully measured for dust cloud parameters, the rotorcraft characteristics and parameters are developed and the dust cloud predictions are calculated. The predicted dust cloud dimensions are developed using the ROTWASH code developed in the FAA Rotorcraft handbook. The original code was written in Fortran and is no longer available electronically. Utilizing the original Fortran 77 code text as well as the detailed development information from Volume I and Volume II of the handbook, the portions of the ROTWASH code critical to this analysis are translated into MATLAB. The text of the code is included in APPENDIX A. Since only relevant ROTWASH subroutines are translated, only the necessary functionality of the original code is fully implemented in MATLAB. That said, each translated function performs all relevant calculations in MATLAB that the equivalent original ROTWASH subroutine performed. The MATLAB code included with this report can be easily translated to any additional programming language as required. This code calculates the predicted dust cloud parameters for one aircraft at one gross weight.

The main function in the FAA ROTWASH code is *pcloud* (Appendix A), which sets and calculates many of the basic values that will be used to predict the overall dust cloud height. After setting the standard day sea level density and using a conversion factor for translating degrees to radians, several case-specific parameters are calculated to allow the program to take into account shaft angles that are not perpendicular to the horizon. Next, the non-dimensional rotor height, the non-dimensional lateral separation for tandem rotors, effective gross weight (including a fuselage downwash factor),

effective disk loading, and the density ratio from standard day sea level conditions are calculated. The next several parameters are utilized by the next function called by *pcloud*, *waljet* (Appendix A).

**Dust Cloud Predictions – Parameter Calculations**

As previously discussed, referencing the 1961 Hiller report, the first critical parameter in dust dynamics is the field maximum dynamic pressure. To determine this maximum dynamic pressure, the entering argument is the location of the beginning of the wall jet, which is the radial position where the maximum static pressure is located. The FAA rotor wash program then utilizes momentum theory, as well as mathematical models from previous research refined to match several previous full-scale flow field experiments, to calculate the location of the maximum and the magnitude of the maximum dynamic pressure.

The FAA ROTWASH program requires an initial guess and an iterative process executed within the MATLAB function *waljet,* found in Appendix A, to calculate the strength and location of the wall jet. First, the initial guess for the radius of the wall jet location (non-dimensionalized by the rotor radius) is set at an initial value of 2:

$$\left(\frac{r}{R}\right)_j = 2.0 \qquad \textbf{(10)}$$

Calculating the location of the wall jet also requires the average induced velocity at the rotor disk, as well as the maximum velocity in the wall jet.

Maximum radial velocity at start of the wall jet is equal to the maximum axial velocity in an equivalent free jet at a distance from the free-jet nozzle exit:

$$\frac{t}{R} = \frac{H}{R} + \left[\left(\frac{r}{R}\right)_j - 1.0\right] \tag{11}$$

This equivalent free jet distance is modified by the wake contraction ratio, which is also presented in *Principles of Helicopter Dynamics* (Leishman, Principals of Helicopter Aerodynamics, 2006, p. 63). This results in the effective slipstream diameter:

$$\frac{t}{D_e} = 0.707\left(\frac{t}{R}\right) \tag{12}$$

The decay function that utilizes the effective slipstream diameter utilizes two functions that are a representation of actual flow field test data results in the maximum surface dynamic pressure:

$$\frac{q_{S\max}}{q_N} = 1.08 - 0.025\left(\frac{t}{D_e}\right)^2 \quad \left\{\left(\frac{t}{D_e}\right) \le 3.5 \tag{13}$$

$$\frac{q_{S\max}}{q_N} = \frac{2.7}{\left(\frac{t}{D_e}\right)} \quad \left\{\left(\frac{t}{D_e}\right) > 3.5 \tag{14}$$

non-dimensionalized by the dynamic pressure of a fully developed slipstream:

$$q_N = \frac{1}{2}\rho_A U_N^2 \tag{15}$$

The maximum surface dynamic pressure is used to calculate the field maximum velocity:

$$\frac{u_m}{U_N} = \sqrt{\frac{q_{s\max}}{q_N}} \qquad \textbf{(16)}$$

(non-dimensionalized by the induced velocity of a fully developed rotor flow at the far wake area) which from momentum theory is related to disk loading and ambient density:

$$U_N = \sqrt{\frac{2DL}{\rho_A}} \qquad \textbf{(17)}$$

Next, a ground effect correction based on test data

$$K_g = 1.0 - 0.9e^{-2\left(\frac{H}{R}\right)} \qquad \textbf{(18)}$$

is combined with the induced velocity of a fully developed rotor to calculate the average induced velocity at the rotor disk:

$$\overline{U} = K_g \frac{U_N}{2} \qquad \textbf{(19)}$$

The process detailed above is iterated until the initial estimate of wall jet radial position converges with the new calculated value:

$$\left(\frac{r}{R}\right)_j = 2.5\sqrt{\frac{\overline{U}}{U_m}} \qquad \textbf{(20)}$$

Some of the above calculations are not readily apparent in the subroutine *waljet* because they are calculated in another of the subroutines and passed as global variables. *Waljet*

also calculates several baseline parameters for additional calculations by the overall ROTWASH program. These are the mean momentum velocity, the non-dimensional height of the half-velocity point in the outer shear layer, and several other constants:

$$\overline{U}_m = \left[ 0.36 \left( \frac{r}{R} \right)_j u_m \overline{U}^{0.14} \right]^{.88} \quad \textbf{(21)}$$

$$\left( \frac{z_h}{R} \right) = \frac{0.65}{\left( \frac{u_m}{\overline{U}_m} \right)^2 \left( \frac{r}{R} \right)_j} \quad \textbf{(22)}$$

$$C_u = \left( \frac{u_m}{\overline{U}_m} \right) \left( \frac{r}{R} \right)_j^1 \quad \textbf{(23)}$$

$$C_y = \frac{\left( \frac{z_h}{R} \right)}{\left( \frac{r}{R} \right)_j} \quad \textbf{(24)}$$

After *waljet* calculates many of the downwash characteristics using previous experimental data, the dimensions of the predicted dust cloud created by the downwash are calculated using the *cloud* function. The calculations of parameters to this point are the baseline for examining any further environmental effects relating to rotor downwash or rotor outflow. As cited previously, the maximum surface dynamic pressure is the critical parameter in determining the amount of terrain erosion. The remaining required value to calculate the effective maximum surface dynamic pressure

$$q_S = \frac{q_{S\max}}{\sqrt{K_t}} \quad \textbf{(25)}$$

is the terrain erosion factor. The terrain erosion factor is calculated

$$K_t = \frac{\overline{D} \rho_P}{D_W \rho_W} \quad \textbf{(26)}$$

or obtained graphically from Figure 12. For this investigation, $K_t$ of 0.025 is used, based on the predominance of particles collected in the full-scale experiment conducted by USVAALABS in 1968 (Ferguson, Rotorwash Analysis Handbook, Volume I: Development and Analysis, 1994, p. 265). Previous experimentation shows that the radial cloud boundary is where the maximum surface dynamic pressure is equal to 1.0 $\frac{lb}{ft^2}$, which results in the maximum radius of the predicted dust cloud:

$$R_C = R\left(\frac{\sqrt{K_T}}{C_3 \frac{1}{2}\rho_A \overline{U}_m^2 C_u^2}\right)^{-0.437} \quad \textbf{(6)}$$

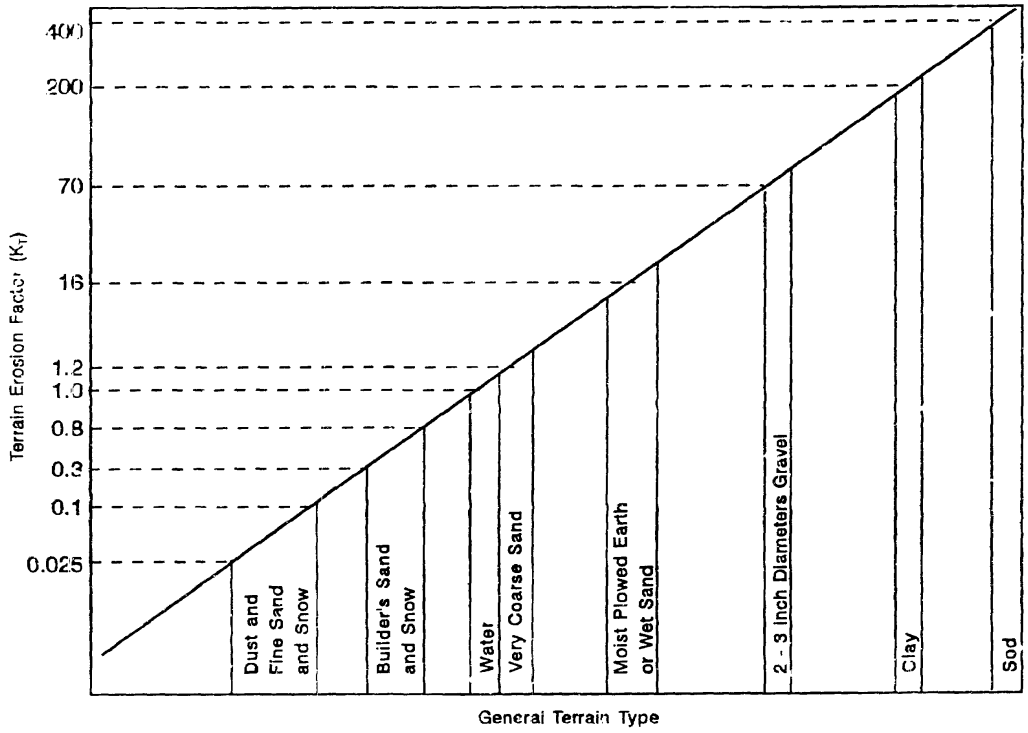


(Ferguson, Rotorwash Analysis Handbook, Volume I: Development and Analysis, 1994, p. 262)

**Figure 12: Approximate Terrain Erosion Factor Values**

where $C_3$ is 1.0 for single rotor aircraft and 2.2 for the distance on the interaction axis of a multi-rotor craft (Ferguson, Rotorwash Analysis Handbook, Volume I: Development and Analysis, 1994, p. 261). To calculate the maximum height of the cloud, a simplified version of vortex roll-up theory, illustrated by Figure 8 and Figure 13, is used. The core of the dust cloud vortex is located at a radial and height location related to the maximum cloud radius:

$$R_V = 0.785 R_C \quad \textbf{(4)}$$

$$Z_V = 0.329 R_C \quad \textbf{(5)}$$

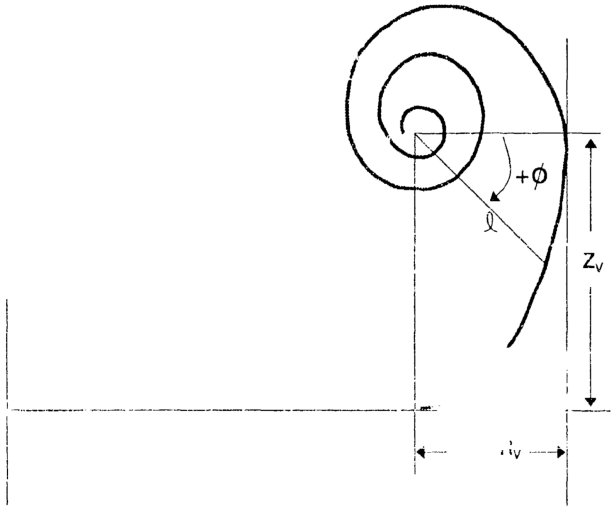


(Ferguson, Rotorwash Analysis Handbook, Volume I: Development and Analysis, 1994, p. 263)

**Figure 13: Logarithmic Spiral Representation of Vortex Rollup**

Given the vortex center location, the maximum cloud height can be calculated by evaluating a logarithmic spiral:

$$\ell = e^{A(\phi+\phi_0)} \tag{27}$$

where, the highest point of the vortex is located at $\phi = -\frac{\pi}{2}$:

$$\ell_V = e^{A\left(-\frac{\pi}{2}+\phi_0\right)} \tag{28}$$

To determine the defining parameters of the spiral, the boundary conditions defined at the center of the vortex, and the distance and angle to the maximum outer cloud radius, are used. The constants are calculated

$$A = \frac{2}{\pi}\ln\left(\frac{Z_V}{R_C - R_V}\right) \tag{29}$$

$$\phi_o = \frac{\pi}{2}\left(\frac{\ln\left(R_C - R_V\right)}{\ln\left(Z_V\right) - \ln\left(R_C - R_V\right)}\right) \tag{30}$$

and when substituted back into equation 28, the result is used to calculate the predicted maximum cloud height:

$$H_C = \ell_V + Z_V \tag{7}$$

The above equations and functions are used to calculate the maximum predicted cloud height and radius for each rotorcraft, and including the interaction axis for multiple rotor aircraft. The results are presented in Table 4.

**Table 4: Predicted Cloud Height By Rotorcraft**

| Rotorcraft | Main Rotor Configuration | Cloud Height (ft) | Cloud Radius (ft) | Interaction Plane Cloud Height (ft) | Interaction Plane Cloud Radius (ft) |
|---|---|---|---|---|---|
| UH-1N | Single | 79.18 | 168.6 | N/A | N/A |
| Lynx | Single | 80.58 | 171.6 | N/A | N/A |
| Tiger | Single | 89.97 | 191.6 | N/A | N/A |
| AH-64A | Single | 109.5 | 233.3 | N/A | N/A |
| UH-60L | Single | 110.1 | 234.4 | N/A | N/A |
| UH-3 | Single | 114.0 | 242.7 | N/A | N/A |
| CH-46D | Tandem | 84.96 | 181.0 | 119.9 | 255.4 |
| Mi-17 | Single | 127.5 | 271.7 | N/A | N/A |
| AW-101 | Single | 139.6 | 297.4 | N/A | N/A |
| CH-53D | Single | 154.5 | 329.1 | N/A | N/A |
| CH-47 | Tandem | 120.9 | 257.5 | 170.6 | 363.4 |
| V-22 | Side-by-Side | 121.3* | 228.4* | 171.3 | 364.8 |
| CH-53E | Single | 100.2 | 213.5 | N/A | N/A |

* Note: V-22 primary cloud predictions are from the nacelles along the y-axis.

To allow comparison between type/model series from these results, in order to show the difference in existing rotorcraft downwash performance, and to qualitatively characterize future designs, the configuration data was used to develop some of the standard characteristic rotorwash numbers. Disk loading (DL), induced velocity ($V_i$), maximum downwash $\left(U_N\right)$, vorticity ($\Gamma$), and the ground vortex strength are several of these parameters. For the analysis, each of these parameters was calculated using data from previous reports or from the user manuals. The disk loading is based on the hovering thrust required to maintain a hover and the area of the main rotor:

$$DL = \frac{T}{\pi R^2} \tag{31}$$

The maximum induced velocity in Equation 1 is velocity induced by the rotor system at the location of the main rotor and is related to the thrust required to maintain a hover, the air density, and the rotor area. The induced velocity is directly related to the maximum downwash velocity:

$$U_N = 2V_i \tag{32}$$

which is the maximum velocity that a given rotor can produce in a hover, assuming a fully developed and unconstrained downwash.

The next several parameters are related, but are non-dimensional parameters. The thrust coefficient is a commonly used parameter to describe the efficiency of a rotor system:

$$C_T = \frac{T}{\rho A(\Omega R)^2} \tag{33}$$

and is related to the hovering thrust, air density, disk area, and the rotor tip velocity squared.

The remaining parameters are dimensional and are centered on describing aspects of the rotational flow that occurs in the rotor downwash. The strength of the tip vortex is dependent on the thrust coefficient and on the rotor tip velocity, as well as a constant k that has been experimentally been determined to be 2.3 (Milluzzo & Leishman, 2010, p. 3). The tip vortex strength is a measurement of the vorticity created by each blade:

$$\Gamma_V \approx kC_T(\Omega R)c \tag{34}$$

The rotor wake strength

$$\Gamma_R = N_B \Gamma_V \quad \textbf{(35)}$$

is related to the tip vorticity but includes the roll-up from multiple blades for each rotor. The tip vortex strength and total wake strength are measured in $\frac{ft^2}{s}$. Additionally, "the rapidity at which the wake vorticies impinge on the ground" (Milluzzo & Leishman, 2010, p. 4) may be used to characterize the rotor downwash:

$$\Omega_S = N_r N_b \Omega \quad \textbf{(36)}$$

Table 5 lists these calculated parameters for the rotorcraft in this study.

**Table 5: Calculated Rotorcraft Parameters**

| Rotorcraft | Disk Loading ($lb/ft^2$) | Induced Velocity (ft/s) | Maximum Downwash (ft/s) | Tip Vortex Strength ($ft^2/s$) | Rotor Wake Strength ($ft^2/s$) | Ground Wake Impingement (Hz) |
|---|---|---|---|---|---|---|
| UH-1N | 4.900 | 35.11 | 70.23 | 525.2 | 1,050 | 10.8 |
| Lynx | 7.021 | 42.03 | 84.07 | 800.3 | 3,201 | 20.3 |
| AH-64A | 10.13 | 50.49 | 101.0 | 1,217 | 4,870 | 19.3 |
| UH-60L | 8.223 | 45.49 | 90.98 | 1,107 | 4,427 | 17.2 |
| UH-3 | 6.183 | 39.44 | 78.89 | 1,058 | 5,288 | 16.9 |
| CH-46D | 4.732 | 34.51 | 69.01 | 1,245 | 3,735 | 26.4 |
| Mi-17 | 6.359 | 40.00 | 80.01 | 1,150 | 5,751 | 16.0 |
| UH-101 | 9.694 | 49.39 | 98.78 | 1,605 | 8,024 | 17.5 |
| CH-53D | 8.990 | 47.56 | 95.13 | 1,688 | 10,130 | 18.5 |
| CH-47 | 7.368 | 43.06 | 86.12 | 2,274 | 6,823 | 22.5 |
| V-22 | 20.38 | 71.61 | 143.2 | 3,565 | 10,690 | 39.7 |
| CH-53E | 12.26 | 55.53 | 111.11 | 1,615 | 11,300 | 21.6 |

## Summary

The results from the historical data, when combined with the observations made in this analysis, give a robust database that relates aircraft characteristics to downwash characteristics, including all full-scale effects and accounting for vorticity. These results enable a comparison of aircraft performance under DVE conditions. Also, designers of new rotorcraft can use these results as a first-order characterization of a new design. Follow on calculations using the MATLAB functions could then be used to produce a more accurate estimate of DVE performance of new designs.

# IV. Results and Analysis

## Assessments of Quality of Data

The results of this analysis are all derived from in-flight data. For the rotorcraft depicted in each individual piece of media, on the given day at the given conditions and configuration, the predictions relate to the cloud that is observed and measured from photographs and video. However, the limitations to the scope of this analysis potentially affect the consistency of the data. Unknown rotorcraft operating weights, unknown altitudes, varying quality of media, and varying density of data points for each rotorcraft, all contribute to some variation in the data used in this analysis. However, it has been shown from previous research that significant variation occurs even in controlled conditions. Previous results of back-to-back runs with identical test configurations, under controlled conditions show deviation on the order of 15% (Rodgers, 1968, p. 4). This indicates that even in a full-scale, comprehensive flight test, variations of measured data are of the same order of magnitude as potential variations caused by the assumptions in this analysis. Finally, data quality variations due to assumptions have been bounded by previous discussion.

In light of natural variation experienced from event to event, sample size is important to increase the confidence level in the results. In this study, some rotorcraft platforms have more data points than others, and some media include better angles allowing for higher quality dimensions. Thus, there is some difference in the data confidence from platform to platform.

Another source of variation in this study is related to the operational maneuvers executed during the recorded images. All media appears to be captured during the hovering or landing phases of flight. In a constant steady state hover, the rotor downwash is fully developed, but during an approach to landing with lower power being developed by the rotor system, effects can vary greatly from one platform to another and from one unit to another with approach techniques. From flight experience, a typical thrust setting for an approach is about half of that required for a steady state hover. Operator training and proficiency, as well as ambient conditions, all affect the results. Also, the ambient winds have an effect on the cloud size, and the cloud from a fast approach is smaller than that of a fully developed hover. Although this uncertainty does impact the results, it affects all platforms in a similar manner. Due to interaction between the ambient winds and forward velocity, by headwinds during landing or approach, there is a built in bias towards a somewhat smaller dust cloud that has not been fully formed. For these reasons, the observed results are expected to be lower than predicted for a fully developed hover. However, since the source of the video is real-life conditions, the observed relationships are valid for the operational use of rotorcraft.

**Consistency of Results**

All data included in this report are consistent with previously published research and data are consistent within this data set. As previously discussed, consistency in the individual media files is addressed by utilizing as many data points as possible, resulting

in the observed dimensions included in Table 6. Dimensions that had only one or two data points were not included.

**Table 6: Observed Dust Cloud Data**

| Rotorcraft | Rise Time (s) | Cloud Height (ft) | Cloud Radius (ft) | Interaction Axis Cloud Radius (ft) |
|---|---|---|---|---|
| UH-1N | 3.2 | 30.53 | 49.59 | N/A |
| Lynx | 2.4 | 19.19 | 35.98 | N/A |
| AH-64A | - | 44.64 | 58.86 | N/A |
| UH-60L | - | 36.04 | 101.9 | N/A |
| UH-3 Mk3 | - | 16.98 | 119.8 | N/A |
| CH-46D | 2.7 | 36.18 | 57.67 | - |
| Mi-17 | - | 39.55 | 100.4 | N/A |
| EH-101 | 3.2 | 31.57 | 94.55 | N/A |
| CH-53D | - | 50.75 | 92.74 | N/A |
| CH-47 | 3.0 | 40.57 | 61.95 | - |
| V-22 | - | 65.85 | 125.0 | 156.8 |
| CH-53E | - | 62.04 | 207.0 | N/A |

**Rating Scale**

Recent Army, Air Force, Marine Corps, and Navy experience in Iraq and Afghanistan demonstrates that the height and breadth of the brownout cloud are important operational factors that are relevant to rotorcraft tactical employment. The operational impacts are primarily related to pilot visibility, which affects safety during takeoff, landing, and troop deployment, especially during multi-ship operations. Detectability of the brownout cloud by opposition forces in a hostile environment is also a concern, but is not specifically analyzed in the scope of this investigation. In order to allow easy characterization and characterization between platforms, it is desirable to have a rotorcraft brownout rating that describes the brownout characteristics or performance.

One approach for this rating is to use basic characteristics of the brownout cloud,

such as those found in Table 6. Either the radius or the height can be used, but each of these dimensions only illustrates a portion of the overall brownout characteristics. Using two or all three measurements is more meaningful, but can cause a question of which parameter is most important. One possible solution is to multiply the dust cloud height and the dust cloud radius to arrive at a brownout area $B$, representative of how much area the dust cloud takes up when viewed from around the helicopter:

$$B = R_C H_C \tag{37}$$

Since the two key design inputs to the ROTWASH program related to size are rotor height and rotor radius, the brownout parameter is non-dimensionalized using the blade radius multiplied by the rotor design height above the ground plane:

$$\frac{B}{HR} = \frac{R_C H_C}{H_B R} \tag{38}$$

This leaves one simple physics-based parameter that is easily calculated.

Robust development of the physics-based approach has several challenges. The first challenge is developing a practical and consistent way to calculate an aircraft baseline for multiple rotorcraft at multiple locations. The second challenge is financial. Development of good data for multiple scenarios is expensive. Finally, for measuring all rotorcraft in consistent environmental conditions for an accurate comparison, special equipment to monitor and measure is required; therefore the physics-based approach is impractical for evaluating tactical considerations in-theater, even by experienced operators.

The next possible solution is not based on quantitative dust cloud measurements, but on quantitative evaluation from the perspective of the pilot. When evaluating a rotorcraft's inherent severity of and susceptibility to brownout, the pilot's perspective is the most critical aspect of the dust cloud characteristics observation. The pilots' views may be different from that indicated by external dust cloud measurements. Therefore, a scale that uses well-defined characteristics that a pilot can observe during a hover, an approach, or a maneuver is desired.

There are several reasons that a precise brownout pilot visibility rating system would be helpful. Operationally, a rating scale would allow units and pilots to arrive at a quantitative evaluation of different tactics to minimize brownout, such as varying the approach angle or airspeed for a no-hover landing. Observation of several cockpit perspective view videos of brownout approaches illustrates clearly that different aircraft have dramatically different DVE characteristics from the pilots' perspective under similar ambient conditions. In development and modernization of existing rotorcraft, a precise scale would allow evaluation of aircraft modifications for improving brownout characteristics. Such a scale could also be used as a specification for new aircraft designs or as a performance standard for brownout mitigating synthetic vision systems.

There is an existing, historically significant scale, that allows for completing a task and quantitatively determining the pilot workload through a pilot assessment, the Handling Qualities Rating (HQR) scale, developed by Cooper and Harper (Cooper, Harper, 1969, p. 12). The HQR scale is specifically tailored for trained pilots using key words in a decision tree to determine the aircraft performance and associated pilot

workload. This is a valid approach that may be simplified in this case to be executable by any fleet pilot.

The brownout rating scale found on page 90 of Appendix B was developed with the methodology, clarity, and simplicity of the HQR scale in mind. It consists of a decision tree that contains questions that are simple enough to be answered by fleet pilots to allow determination of the brownout rating. The main drawback of this scale is that it presumes that the first visual cue that a pilot will lose is the horizon, and the last visual cues lost are the near field cues. This indicates that an enhancement should be developed; one that can take into account both horizon cues and near field cues, but that also results in only a single brownout metric.

To provide characterization of multiple Type/Model/Series qualities in DVE, a comparison based on an accepted design standard is desirable. Aircraft Design Standard 33 (ADS 33) includes criteria for degraded visual environments as well as a visual acuity scale (U. S. Army Aviation and Missile Command, 2000, p. 74). These criteria and scales are designed for specially trained pilots where all the visual cues required for a maneuver can be clearly seen. These standards are not appropriate for evaluating maneuvers where all visual reference might be lost. Modification is required to account for untrained pilots and to focusing the evaluation on the visual aspects of the DVE.

To take DVE into account, utilizing the scales contained in ADS 33, as well as the general methods used to evaluate handling qualities with the Cooper Harper Rating Scale, a new scale was developed and is shown in Figure 14. The simple and clear questions that guide the pilot to selecting a rating for the horizon cues and near field cues can be

found on page 90 in Appendix B. This scale compiles the rating of the horizon cues and the near field cues by plotting both on Figure 14. The plotted point is located in a distinct


**Figure 14: Brownout Visual Cue Levels**

Brownout Rating Level, designated one through three. This scale will allow comparison of one maneuver to another, or one aircraft to another, for evaluation of the brownout characteristics from the pilot seat using the full details from Appendix B.

Both brownout rating scales included in Appendix B are designed with simple and clear questions that average operational pilots can answer clearly during any maneuver that might be affected by brownout, including hover, approach to landing, and takeoff. Also included in Appendix B on page 89, is a questionnaire that should be used to collect all the relevant ambient conditions so that the results of the rating can be compared to predictions and previously identified relationships.

**Rotorcraft Background**

The rotorcraft analyzed in this report have characteristics listed in Table 4. For characterization of brownout for each aircraft, it is desirable to first develop the disk loading for each Type/Model/Series. Based on all of the previous research and subsequent analysis, the disk loading is a primary factor in the downwash and dust cloud. Figure 15 includes all the rotorcraft and their associated disk loadings based off the

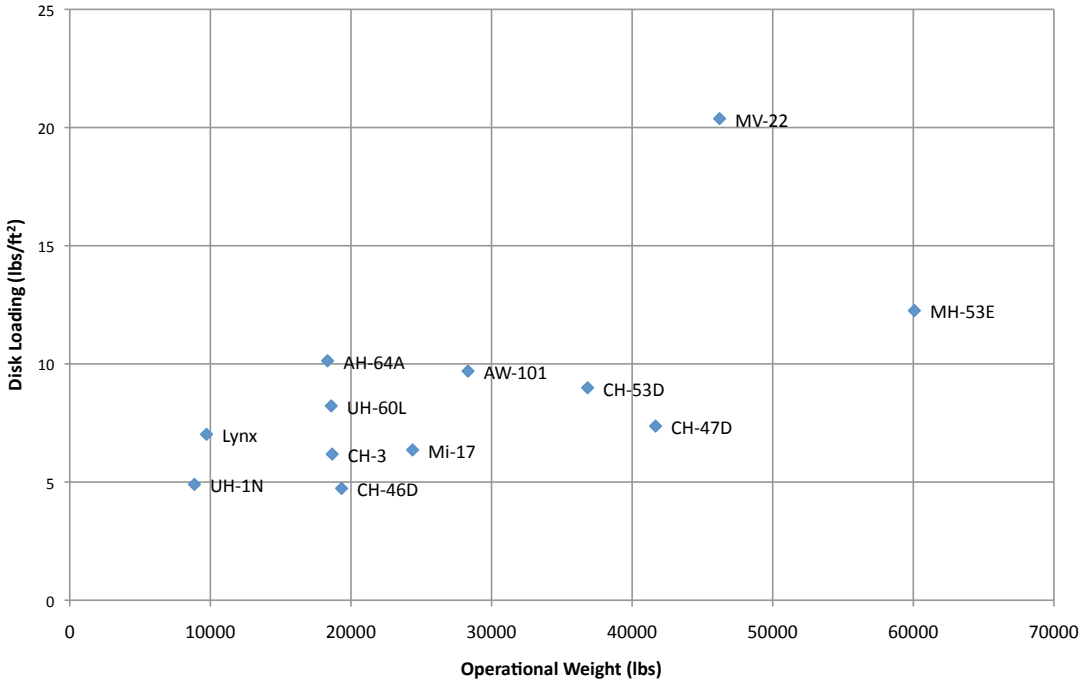


**Figure 15: Disk Loading vs. Gross Weight**

calculated operational weights. Note that number of rotors does not necessarily affect disk loading, however, the traditional dual rotor helicopters (H-46 and H-47) have a lower disk loading than single rotor helicopters of a similar gross weight, while the V-22 has a higher disk loading than single rotor helicopters of a similar gross weight. The high

V-22 disk loading is due to the prop-rotor optimization for forward flight in the propeller configuration, which compromises performance in the hover configuration, resulting in the highest disk loading of the group.

## Synthesis

Each of the rotorcraft analyzed has a range of operating weights. Since the rotor characteristics are fixed, each operational weight corresponds to an associated disk loading. The disk loading for the maximum and minimum weights, as well as the previously defined operational weight are included in Figure 16.

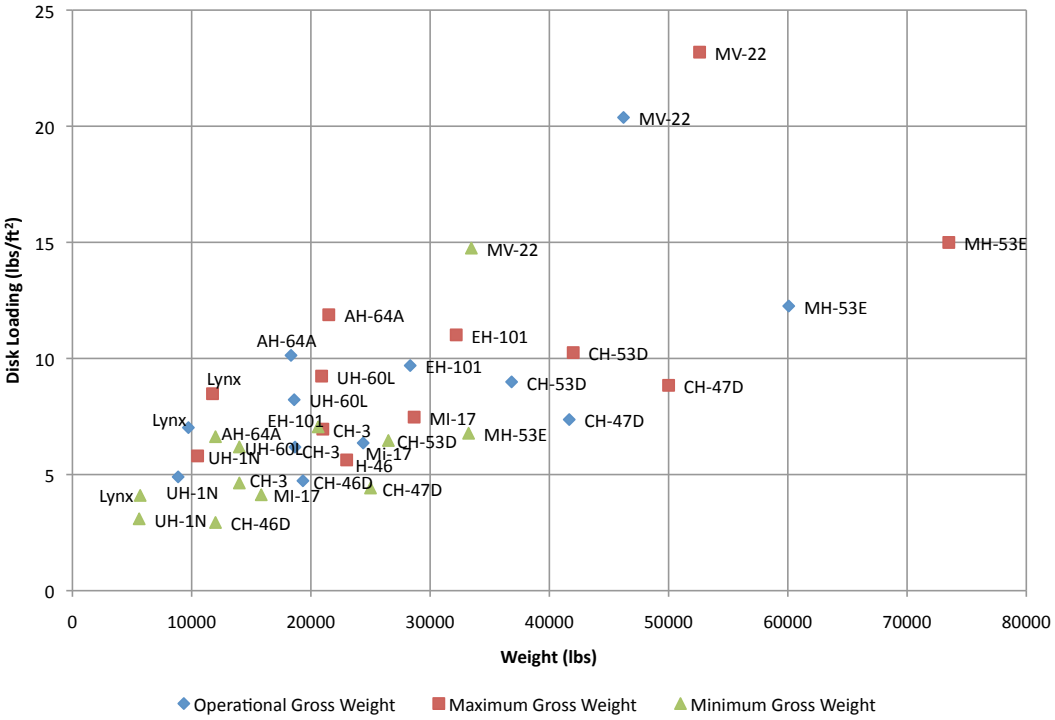


**Figure 16: Disk Loading vs. Gross Weight Range**

The wide range of disk loadings present is apparent. Again, note that the MV-22 exhibits by far the highest disk loading of any of the rotorcraft. As described already, this is

because the prop-rotors are much smaller due to the optimization for forward flight. By contrast, the other two multiple rotor aircraft, the CH-47 and the CH-46, are among the lowest disk loading for their weights. Of note, the EH-101, anecdotally praised for good brownout performance, has a high disk loading for the weights at which it operates (Leishman, 2009). All non-dimensional radius and height data are non-dimensionalized with the rotor radius unless otherwise stated.

To indicate trends in the predicted and observed data, many of the graphs include a trend line. In nearly all cases, a linear fit was applied using the Microsoft Excel 2008 least squares TREND function for each data series included in the figure. Additionally, the square of the Pearson product moment correlation coefficient, $R^2$, is included for each line to indicate the fit quality of the trend line. As the value of $R^2$ increases towards 1.0, the quality of the fit increases.

**Disk Loading Characterization**

The primary analysis is completed on the outer dust radius due to the quality and quantity of the media available, resulting in the most robust data set. The outer dust cloud radius measurements fall below the model predictions as shown in Figure 17. This is expected, because the model predictions are based on ideal steady state, fully developed downwash. Due to the safety risks involved in the dust cloud, real world operational use of rotorcraft rarely involves operations in which a fully expanded dust cloud has time to develop. The observed data reflects this reality and the model does not. The observed dust radii are approximately 50% of the predicted values, and the direct

relationship is also about 50% of the prediction. $R^2$ values indicating the accuracy of the linear fit show are 0.54 for the prediction and 0.40 for the observed data. When the

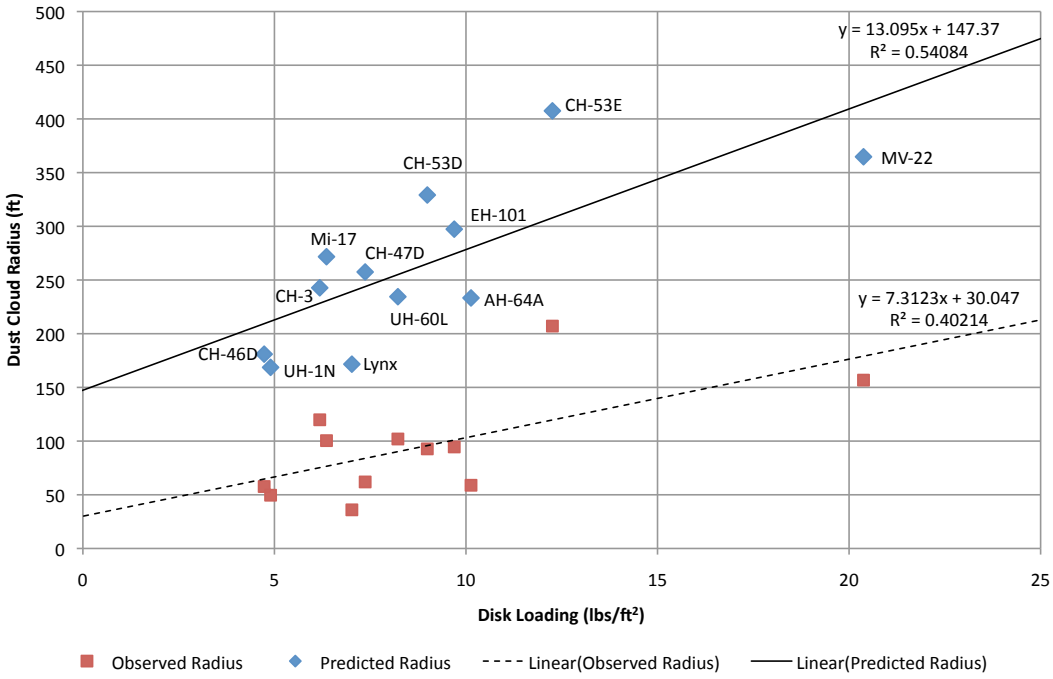


**Figure 17: Dust Cloud Radius vs. Disk Loading**

predicted and observed dust cloud radii are non-dimensionalized by the rotorcraft rotor radius in Figure 18, there is a visually a much stronger relationship between the data points and the trend line. The $R^2$ values for the non-dimensional dust cloud radius linear trend line are 0.95 for the predicted values and 0.78 for the observed data. This indicates that the non-dimensional dust radius is directly related to the disk loading.

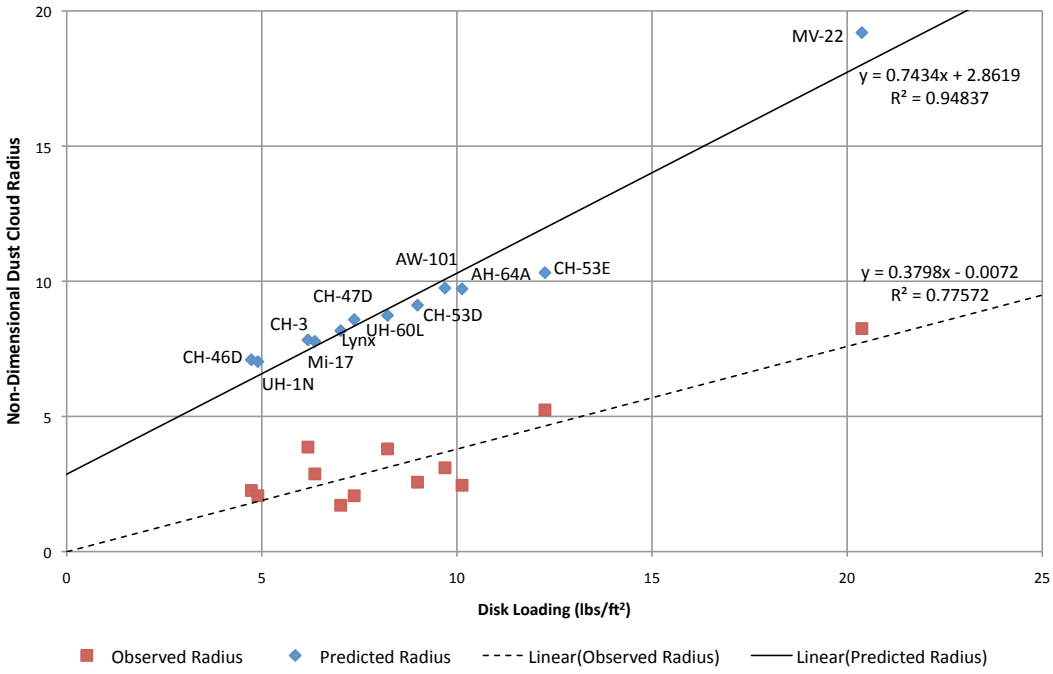


**Figure 18: Non-Dimensional Dust Cloud Radius vs. Disk Loading**

The data for the dust cloud height shows similar relationships to the disk loading as the outer dust cloud radius. In Figure 19, the observed dust cloud height is directly

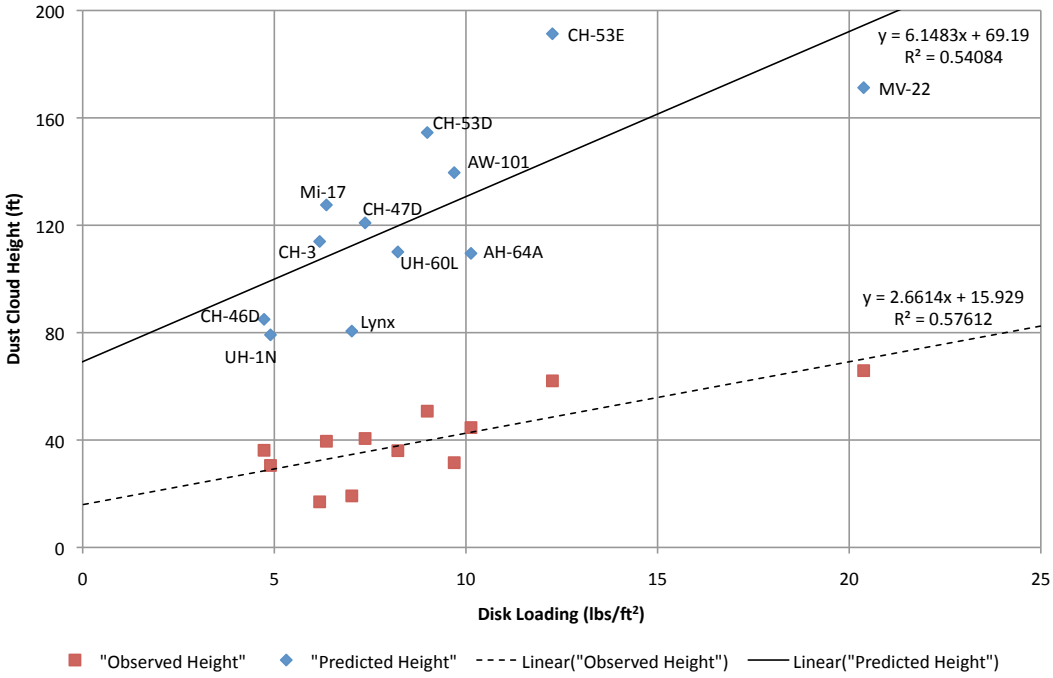


**Figure 19: Dust Cloud Height vs. Disk Loading**

related to the disk loading. Like the dust radius, the $R^2$ values are very similar, but the observed height is closer to 33% of the predicted height. When non-dimensionalizing the dust cloud height, as with the dust cloud radius, the observed and predicted heights data points separate, and $R^2$ values increase to 0.95 and 0.75, as seen in Figure 20.

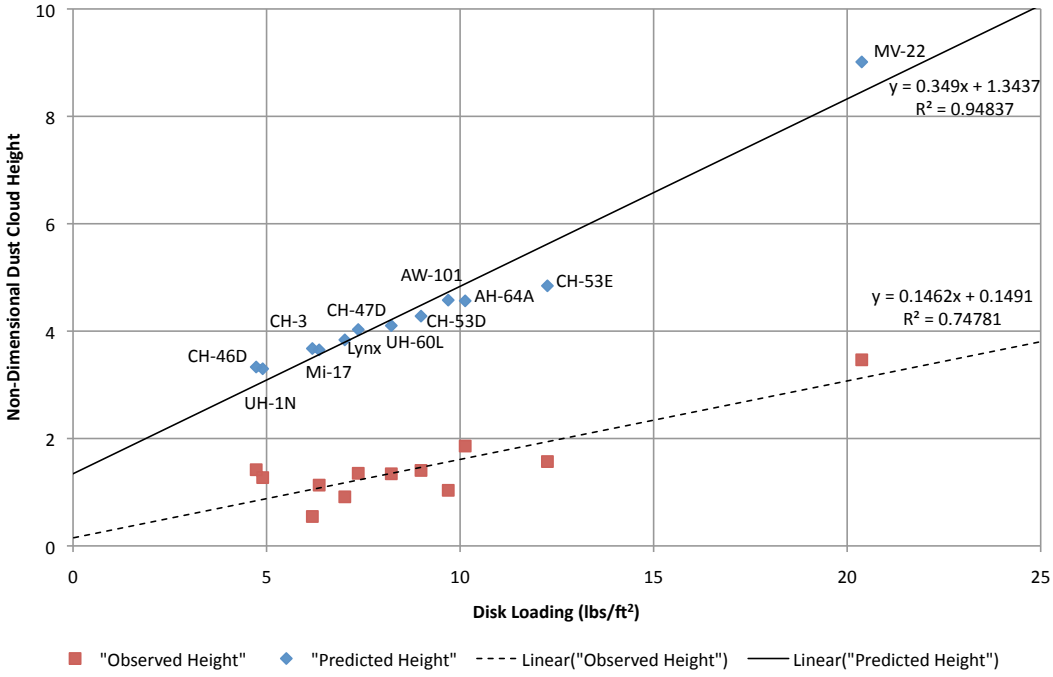


**Figure 20: Non-Dimensional Dust Cloud Height vs. Disk Loading**

## Downwash Velocity

The velocity of the downwash created by a given rotor is linearly related to the disk loading, so plotting the relationships between the downwash velocity and dust cloud characteristics, as expected, show a similar relationship to that demonstrated by the disk loading. Figure 21 shows that the relationship between the downwash velocity generated by the rotor disk and the dust cloud radius has similar $R^2$ values to those of the disk

loading data sets. Like the disk loading and the observed radius data set, the relationship between the downwash velocity to the radius of the dust cloud has much higher $R^2$

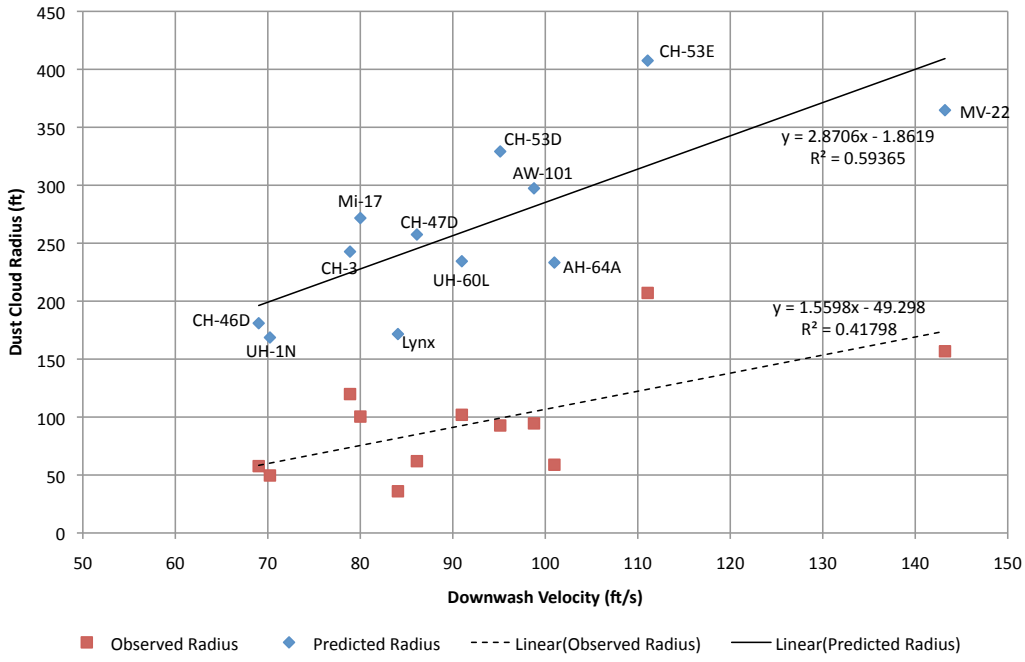


**Figure 21: Dust Cloud Radius vs. Downwash Velocity**

values when non-dimensionalized with the rotor radius in Figure 22. Both the

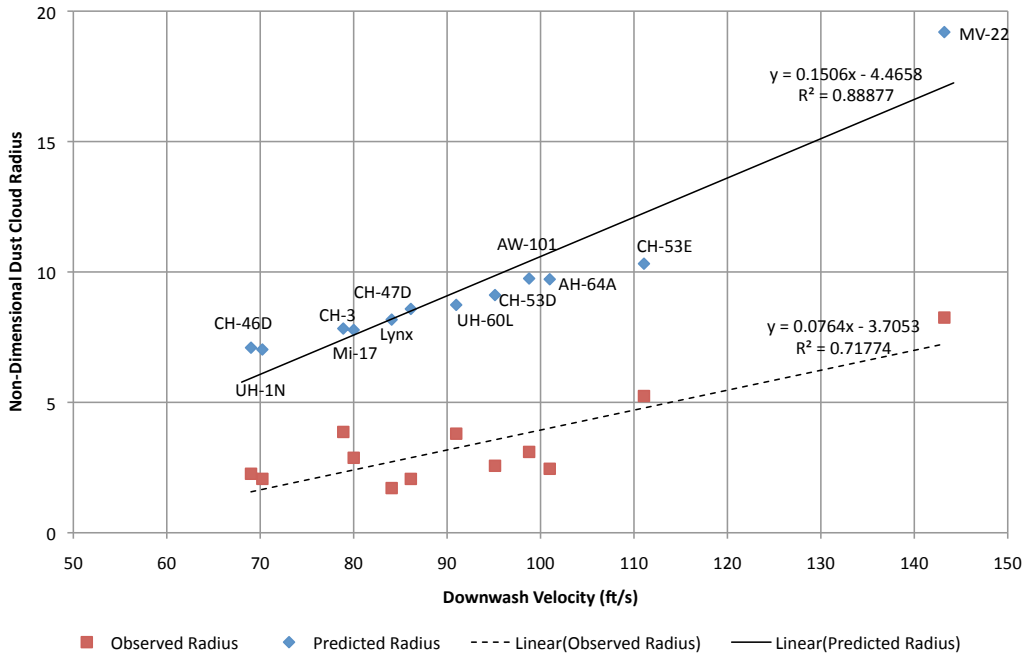


**Figure 22: Non-Dimensional Dust Cloud Radius vs. Downwash Velocity**

predicted radius $R^2$ value and the observed $R^2$ value are slightly less than the non-dimensional $R^2$ values calculated for the disk loading relationship to dust radius. Examining the relationship of the height of the dust cloud to the maximum downwash velocity in Figure 23 has similar results to that of disk loading when relating

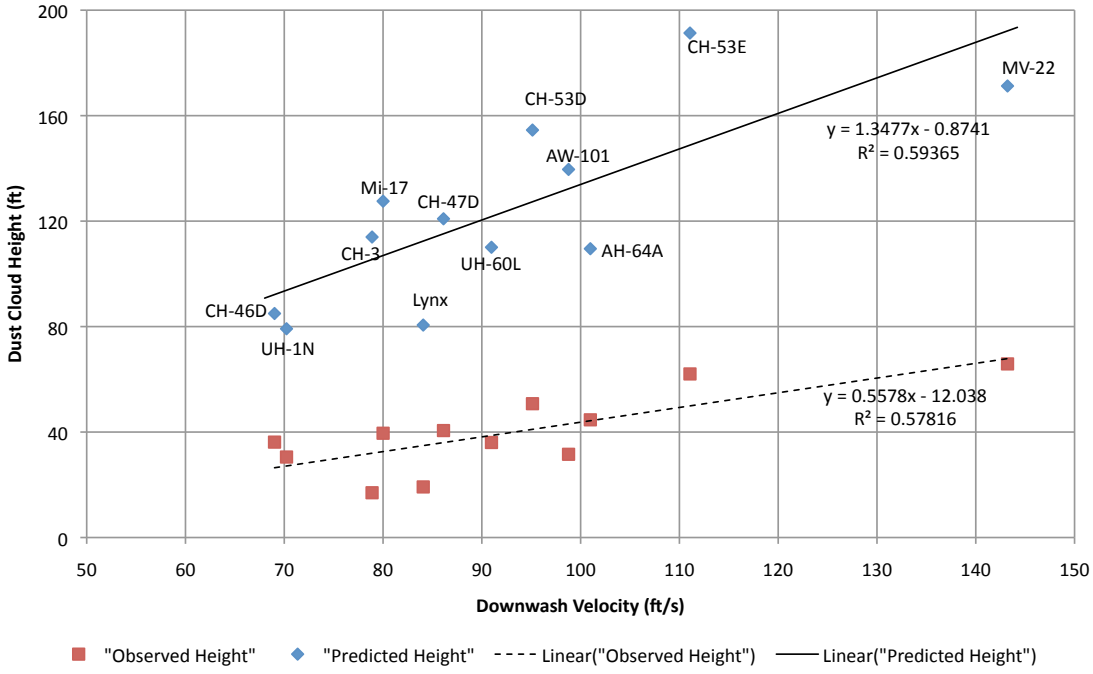


**Figure 23: Dust Cloud Height vs. Downwash Velocity**

the dust height. Once the data are non-dimensionalized in Figure 24 by $R$, the $R^2$ values are slightly less than the $R^2$ values of the disk loading analysis.

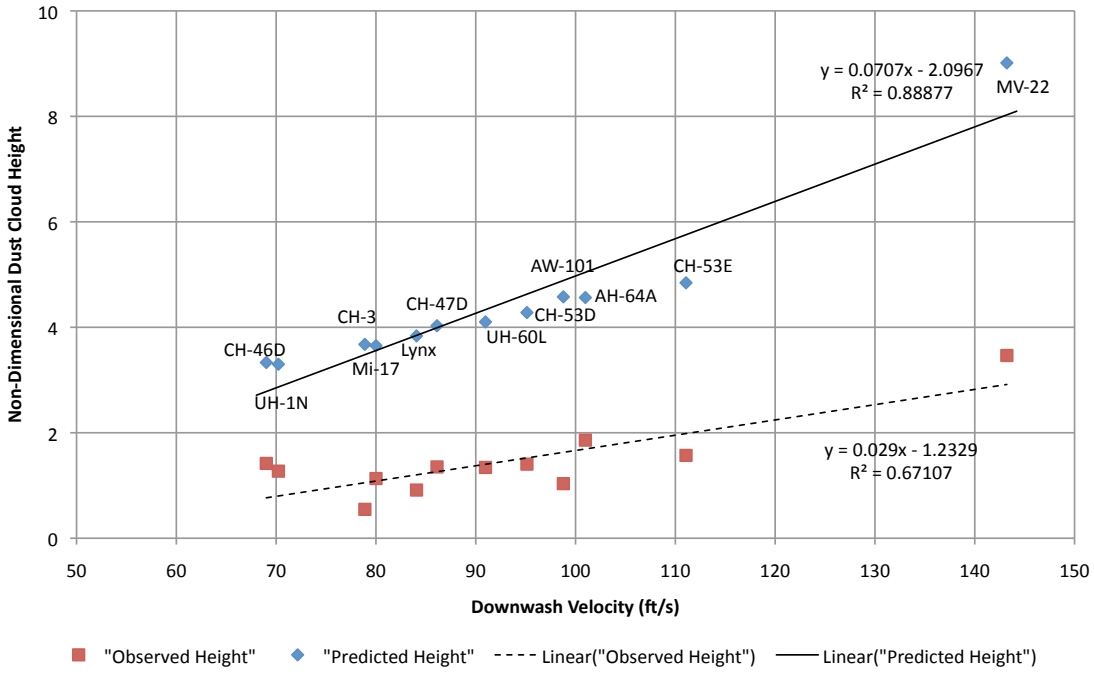


**Figure 24: Non-Dimensional Dust Cloud Height vs. Downwash Velocity**

## Tip Vortex Strength

The tip vortex strength is related to the disk loading and the rotor tip speed. This results in a parameter that is heavily influenced by design choices. However, when the tip vortex strength is compared to the dust cloud radius and plotted in Figure 25, the $R^2$

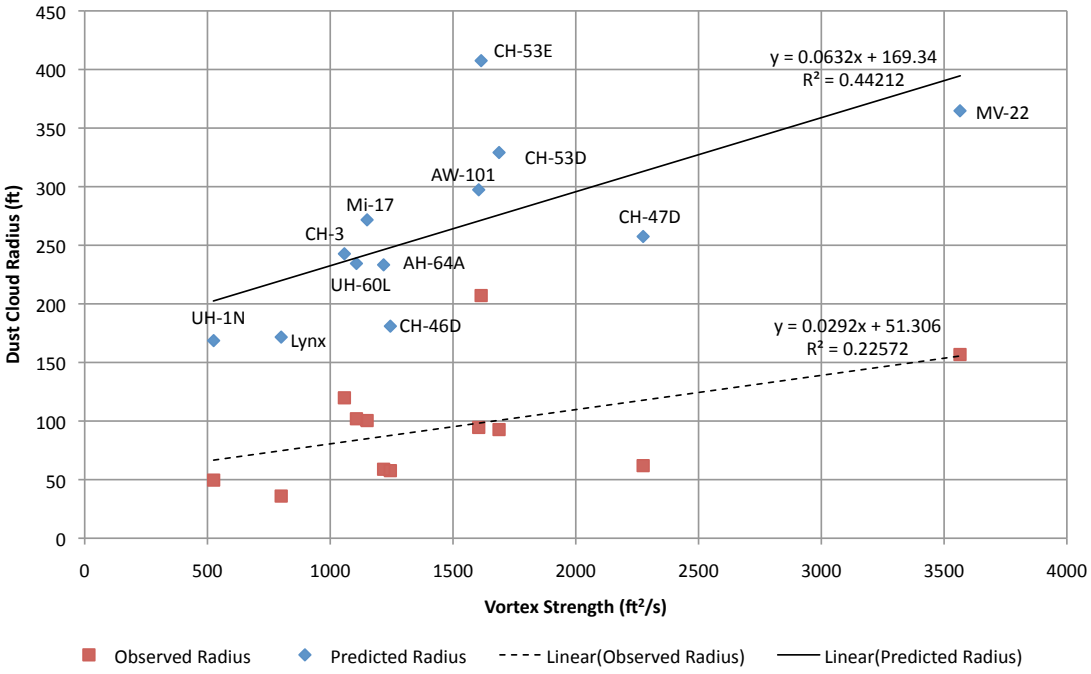


**Figure 25: Dust Cloud Radius vs. Tip Vortex Strength**

values are only 0.44 and 0.23. This is significantly lower than previous results. When non-dimensionalized in Figure 26, the $R^2$ values are increased to 0.77 and 0.55, which are much less than the corresponding non-dimensional disk loading related parameters. When the tip vortex strength is instead compared to the dust cloud height in Figure 27, the $R^2$ values indicate a stronger relationship between the dust cloud height and the tip vortex strength than the dust cloud radius, but overall the tip vortex strength still shows lower $R^2$ values than previously examined parameters.

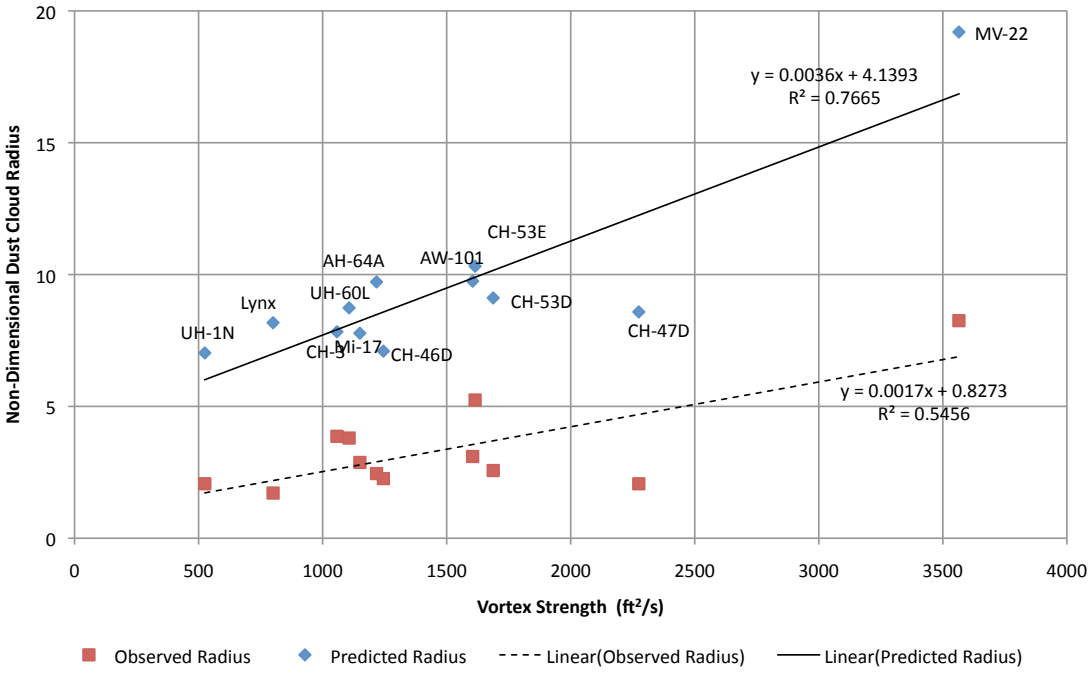


**Figure 26: Non-Dimensional Dust Cloud Radius vs. Tip Vortex Strength**

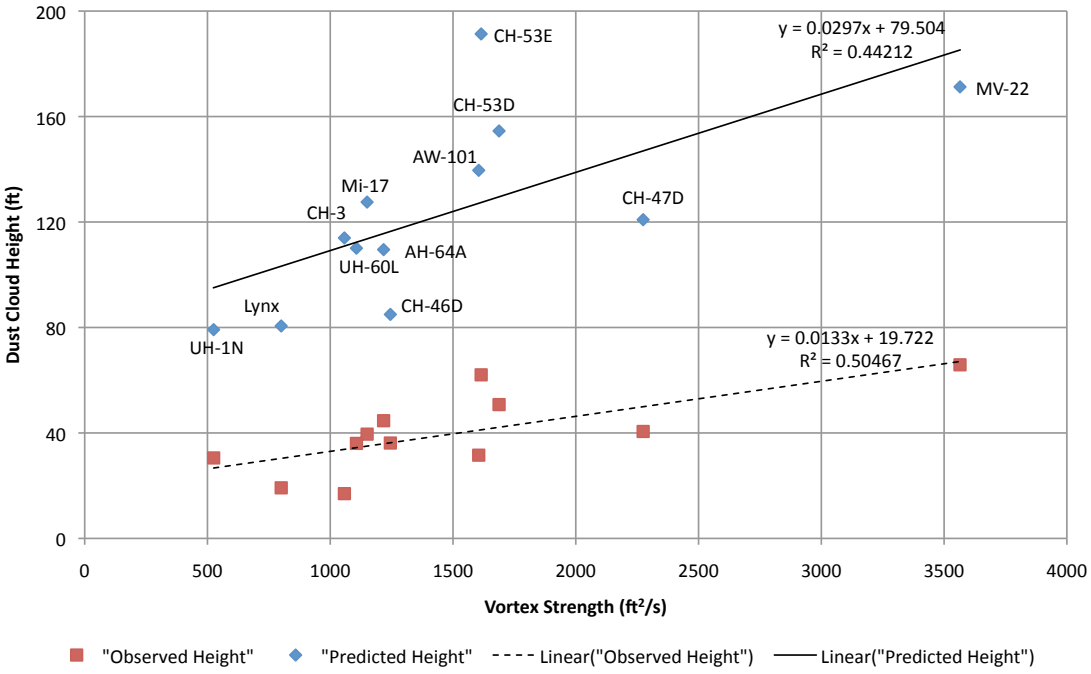


**Figure 27: Dust Cloud Height vs. Tip Vortex Strength**

When non-dimensionalized in Figure 28, the dust cloud height and relationship to rotor $R^2$ values are 0.77 for the predicted dust cloud height and 0.64 for the observed dust cloud height.

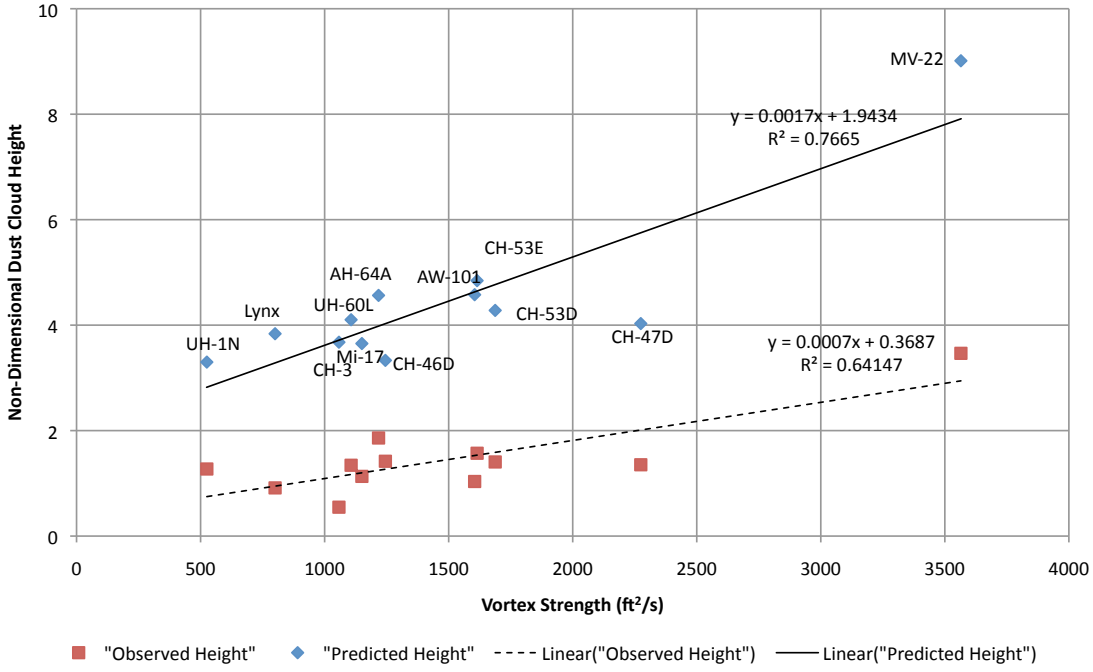


**Figure 28: Non-Dimensional Dust Cloud Height vs. Tip Vortex Strength**

## Rotor Wake Strength

The rotor wake strength is related to the tip vortex strength but includes the number of blades in each rotor. When the rotor wake strength is compared to the predicted and observed cloud radius in Figure 29, the $R^2$ values are 0.94 and 0.60 for the dimensional numbers. The predicted dust radius almost matches the highest $R^2$ value for the relationship between the non-dimensional disk loading and the dust cloud radius, but the observed $R^2$ value is significantly lower than the 0.78 of the disk loading observation.

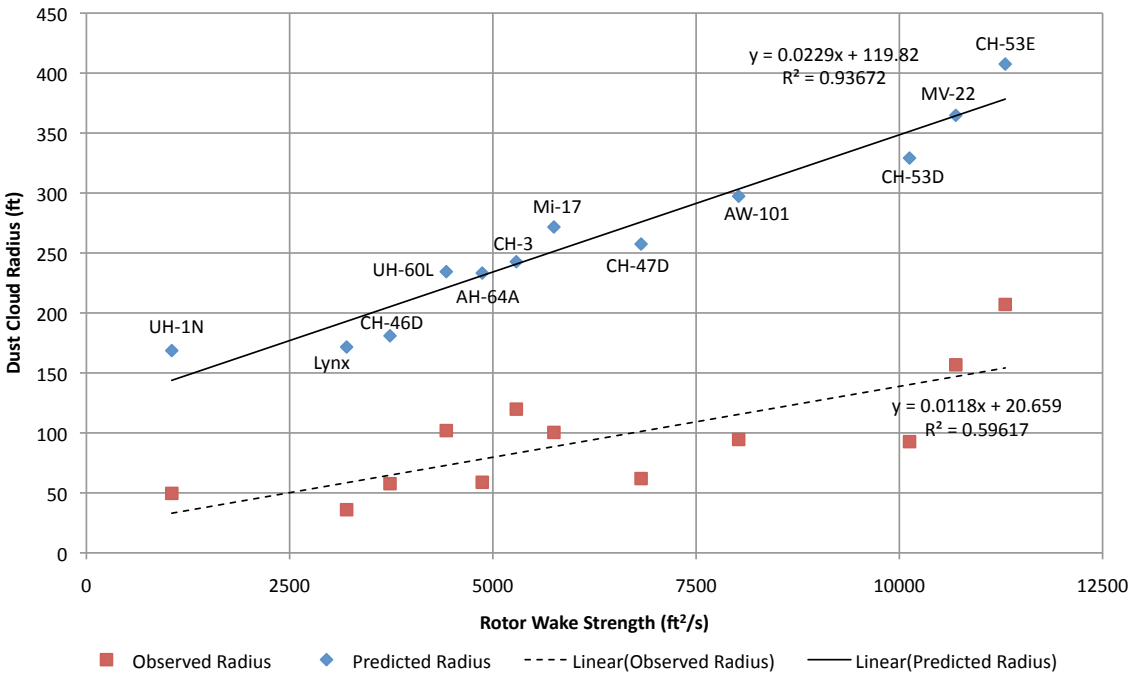


**Figure 29: Dust Cloud Radius vs. Rotor Wake Strength**

When the relationship between the rotor wake strength and the non-dimensional dust cloud radius is plotted in Figure 30 $R^2$ values of 0.40 and 0.42 are among the lowest

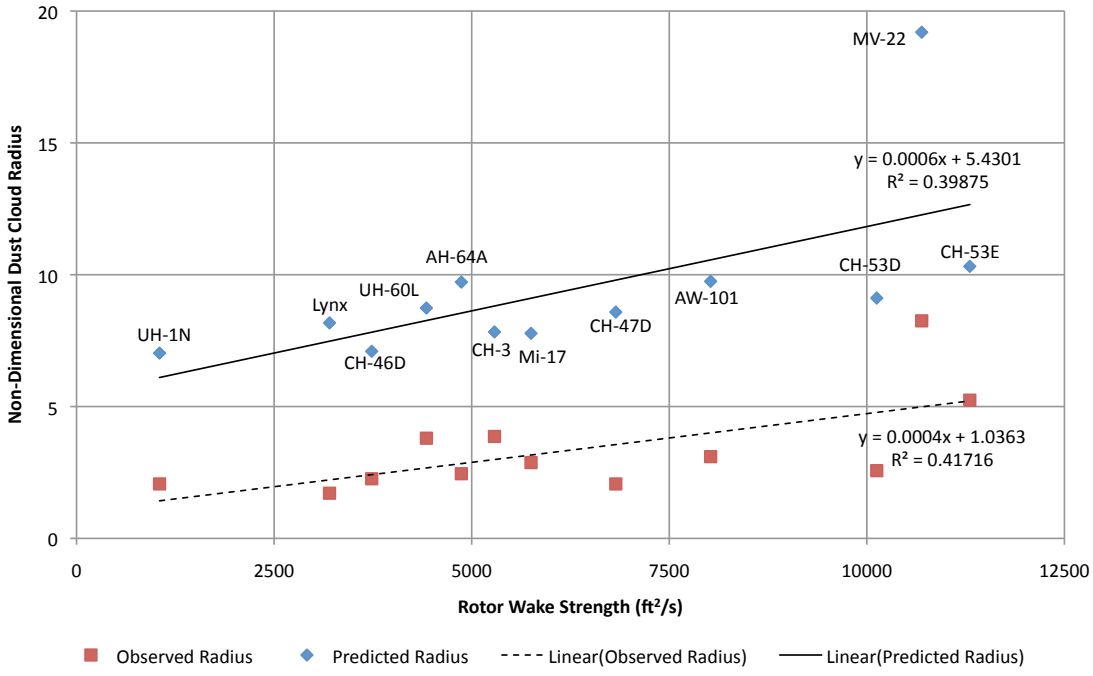


**Figure 30: Non-Dimensional Dust Cloud Radius vs. Rotor Wake Strength**

analyzed. When the rotor wake strength analysis is conducted with the dust cloud rotor height in both dimensional (Figure 31) and non-dimensional (Figure 32), the results are nearly identical to the radius analysis.

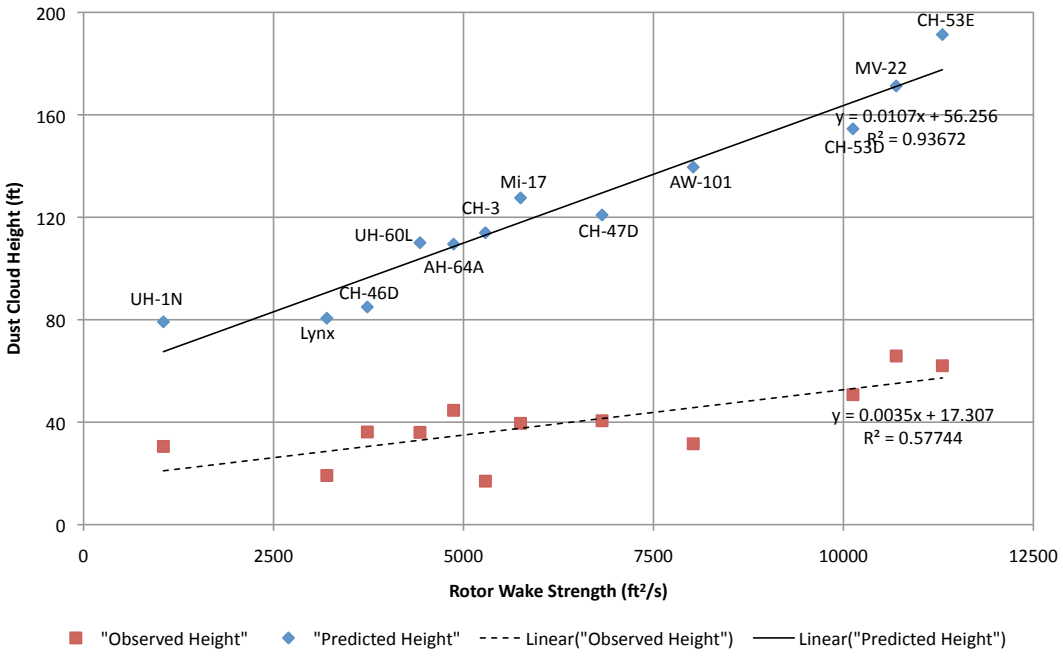


**Figure 31: Dust Cloud Height vs. Rotor Wake Strength**

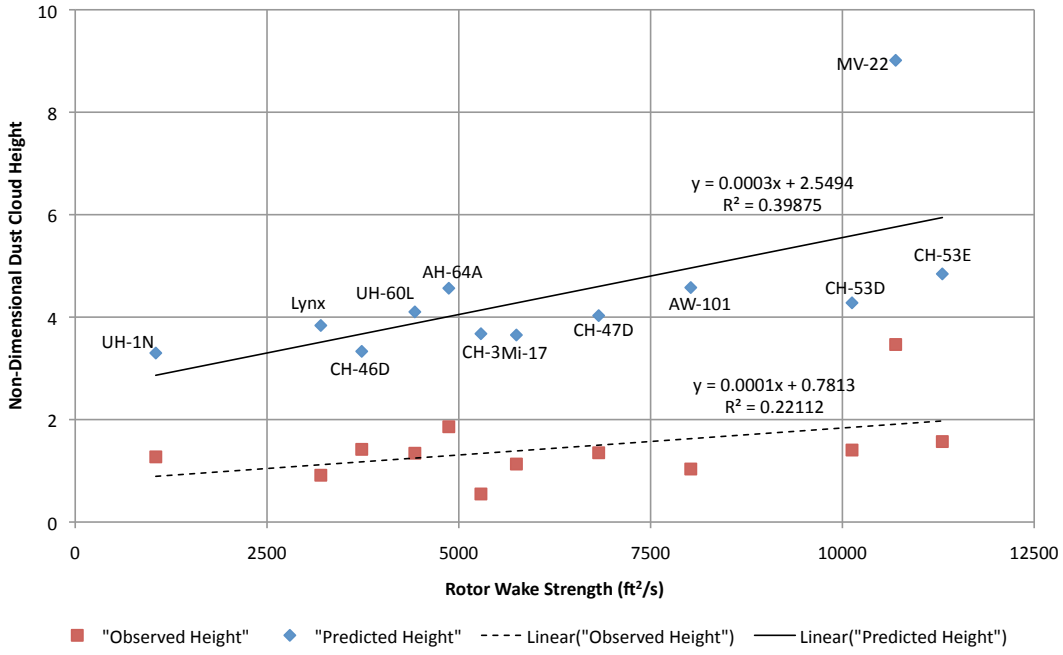


**Figure 32: Non-Dimensional Dust Cloud Height vs. Rotor Wake Strength**

## Ground Wake Impingement

The ground wake impingement is a measure of how often a vortex impacts the ground based on the number of blades, the number of rotors, and the speed at which the rotors are circulating. The relation ship between the dimensional dust cloud radius and the ground wake impingement is weak when shown in Figure 33 with $R^2$ values of only

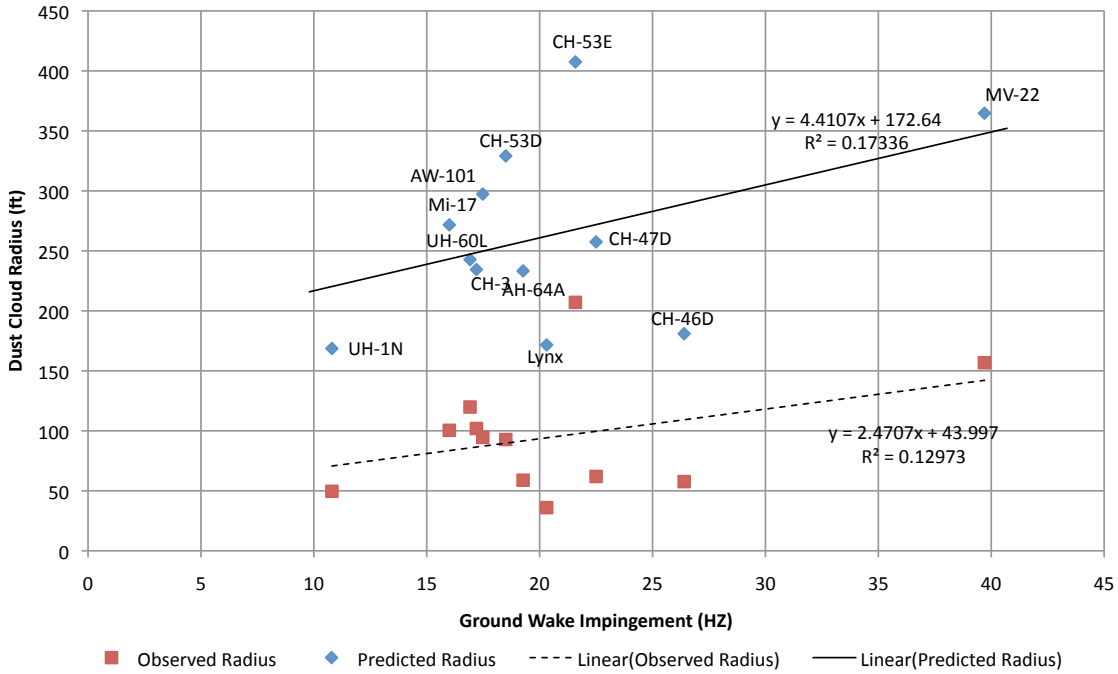


**Figure 33: Dust Cloud Radius vs. Ground Wake Impingement**

0.17 and 0.13 for the predicted and observed values respectively. When non-dimensionalized in Figure 34, the $R^2$ values are somewhat increased to 0.69 and 0.50 for

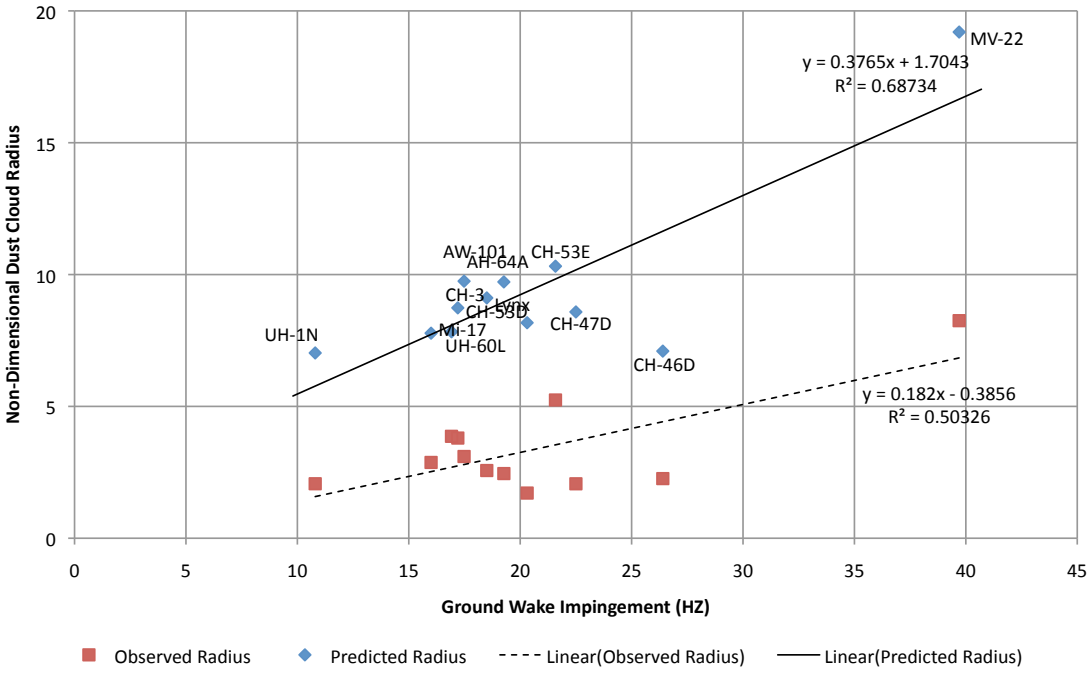


**Figure 34: Non-Dimensional Dust Cloud Radius vs. Ground Wake Impingement**

predicted and observed respectively. The predicted and observed $R^2$ values are significantly lower than the top matching parameters. The plots for the dust cloud height are not included because the relationships closely match the radius, with identical $R^2$ values for the predictions, and only marginally higher $R^2$ values for observed height of 0.35 for dimensional and 0.67 for non-dimensional.

## Additional Analysis

The brownout area was discussed previously as a possibility for a parameter to provide a single number indicating the brownout characteristics for a rotorcraft. In Figure 35, the non-dimensional brownout area is plotted with the best linear fit data set,

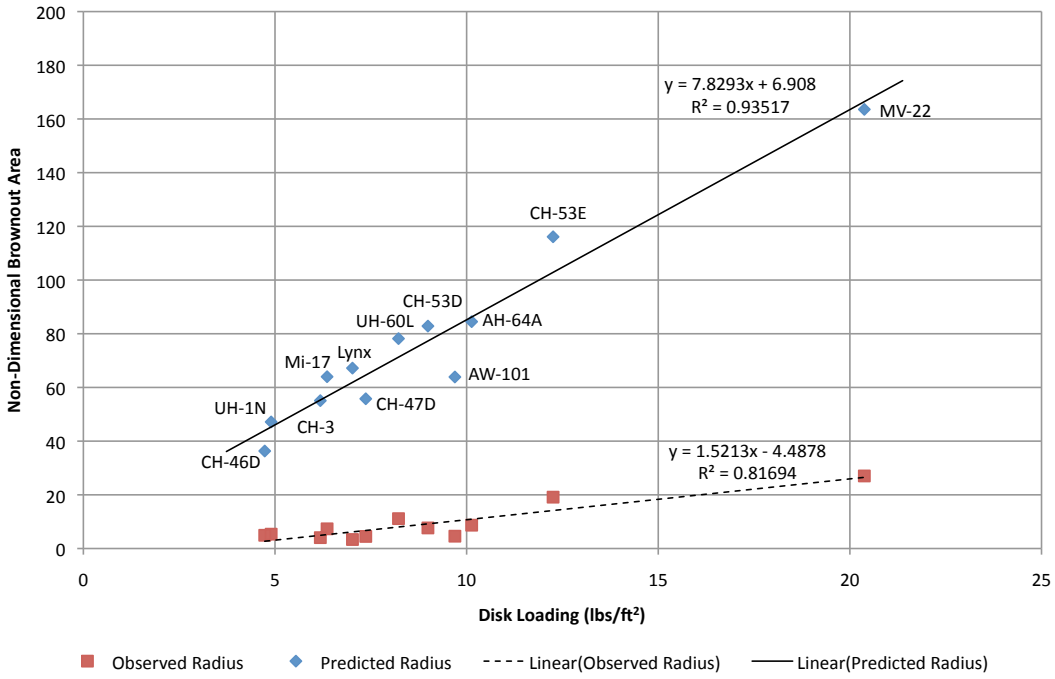


**Figure 35: Non-Dimensional Brownout Area vs. Disk Loading**

disk loading. This brownout area does have high $R^2$ values, with the predicted $R^2$ value of 0.94 nearly matching that of the highest $R^2$ value, 0.95, and the observed data $R^2$ value the highest in the analysis, 0.75

The final parameter that may indicate a relationship to the dust cloud size is the rotor thrust coefficient ($C_T$). When plotted in Figure 36, the $R^2$ values are low, only 0.64

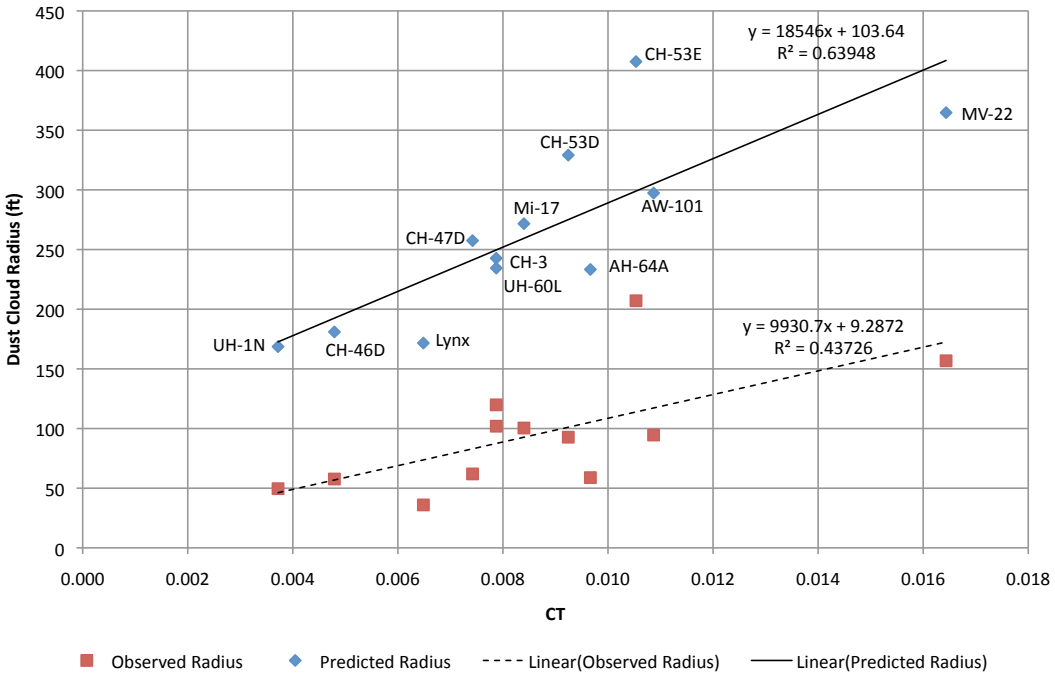


**Figure 36: Dust Cloud Radius vs. Thrust Coefficient**

and 0.44. When the dust cloud radius is non-dimensionalized in Figure 37, the $R^2$ values increased to 0.82 and 0.70, but they are somewhat lower than analysis compared to the disk loading.

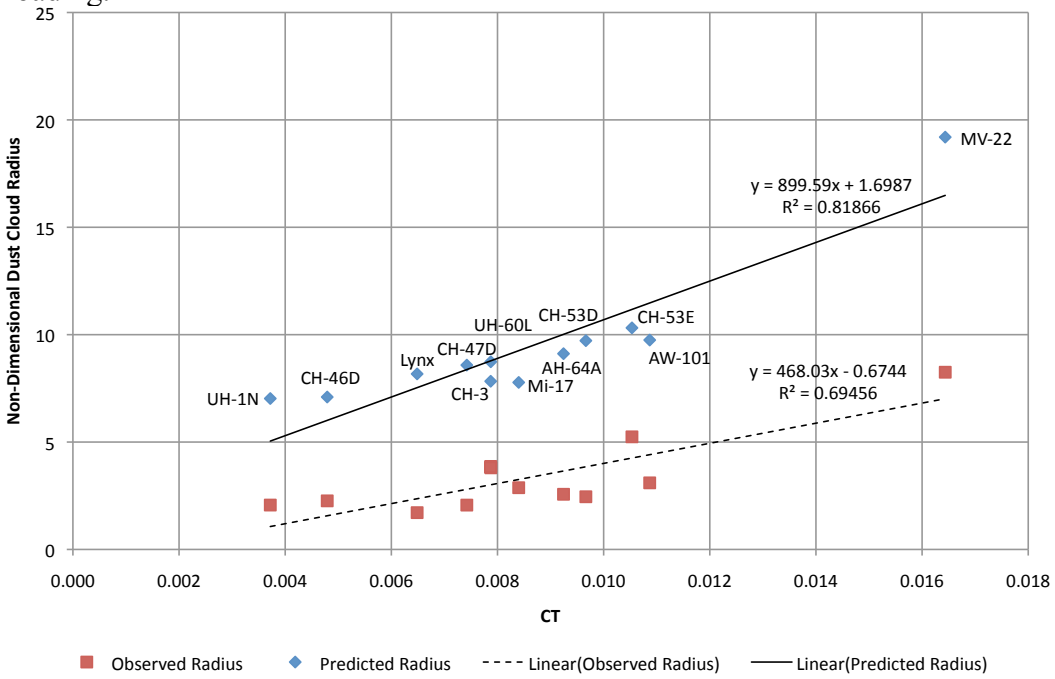


**Figure 37: Non-Dimensional Dust Cloud Radius vs. Thrust Coefficient**

When graphed, the some of the individual data points for the V-22 appear to contrast with other rotorcraft, even from the other multiple main rotor aircraft. Both the dust predictions and observations for the V-22 fall far from the trend line in some of the previous graphs such as Figure 22 and Figure 24. All the results graphed to this point are referenced to the dust cloud along the x-axis. As explained when defining the frame of reference, aircraft with multiple rotors have an interaction plane where the rotorwash from the independent rotors interacts. There are three multi-rotor aircraft analyzed, however, the H-47 and H-46, have traditional downwash and outflow along the y-axis since the interaction plane includes the y-axis and z-axis. The interaction plane of the V-22 includes the x-axis and z-axis, and affects the downwash and outflow along the x-axis. Therefore, the observed and predicted cloud measurements are likely higher because of the increased flow of the interaction plane. To evaluate whether this data has an effect on the curve fit, Figure 38 and Figure 39 are examples with the V-22 data removed and corrected curve fit applied.

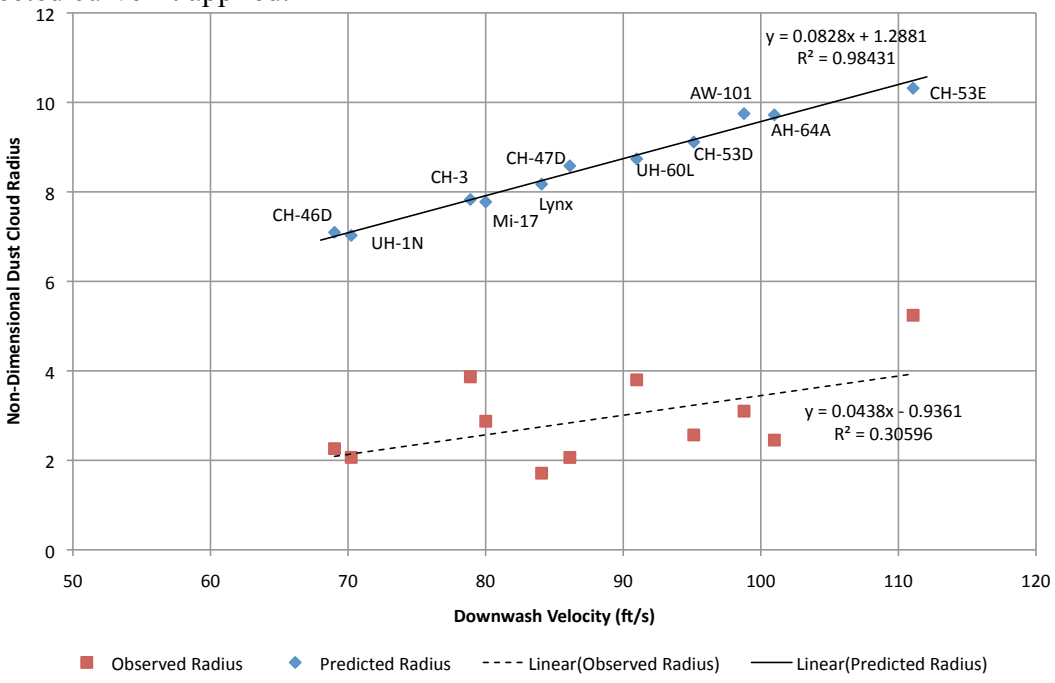


**Figure 38: Non-Dimensional Dust Cloud Radius vs. Downwash Velocity**

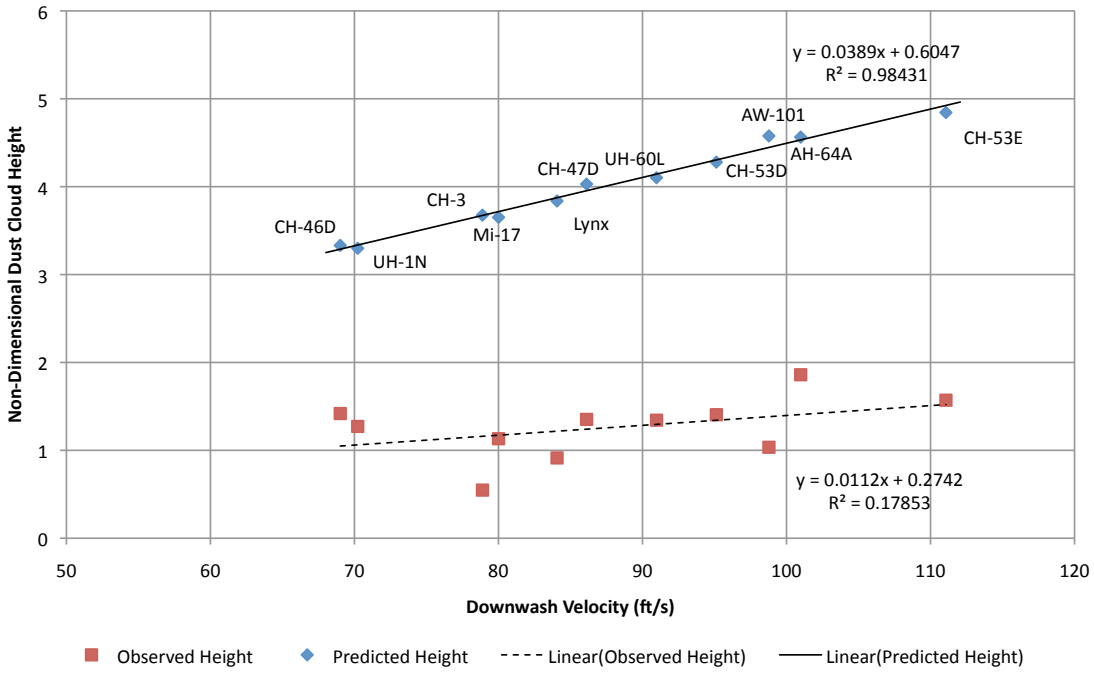


**Figure 39: Non-Dimensional Dust Cloud Height vs. Downwash Velocity**

Without the V-22 included, the predictions based on the downwash velocity for non-dimensional dust radius and dust height fit much better, resulting in increased $R^2$ values from 0.88 to 0.98 for Figure 38 and Figure 39. However, the observed data $R^2$ values decrease from 0.72 to 0.31 for the dust radius and from 0.67 to 0.18.

An additional important observation can be seen in many of the figures, including Figure 22. Of the 12 rotorcraft data points plotted, 10 of the observed data points match the location of the predicted data points when compared to which side of the curve fit the data point is on (if the prediction is above the curve fit, the observed is above the curve fit). This indicates that some future analysis may determine a more direct relationship than the disk loading.

## Dust Cloud Rise Time

Following are additional figures illustrating the rise time for the dust cloud. With so few data points, it is difficult to draw conclusions. Figure 40 shows how the rise time

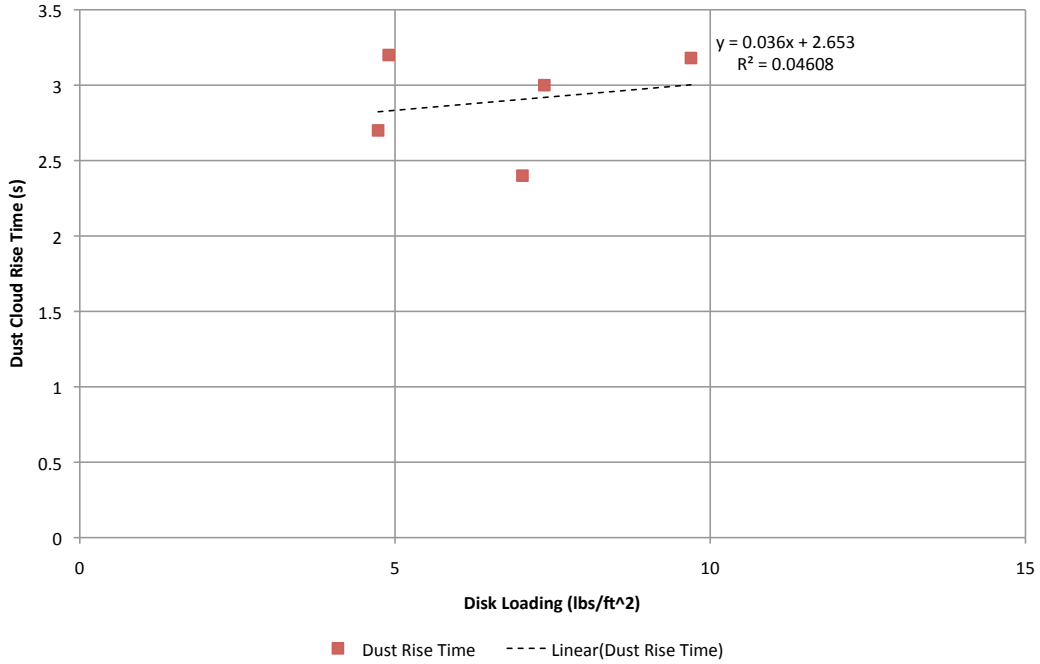


**Figure 40: Dust Cloud Rise Time vs. Disk Loading**

relates to the disk loading. With no software predictions there is no model to compare to and initial analysis does not indicate a strong relationship between disk loading and the dust cloud rise time. More data is needed to draw a conclusion.

## Adjusting for Low Power

In all the preceding Figures, the observed dust radius and height is generally only 25% to 50 % of the predicted values. As discussed previously, this is due to the operational nature of the maneuvers during which the data was collected, which use decreased power settings and transient condition. In attempt to examine whether utilizing an approach power setting (half the thrust of a standard hover) in the prediction will

reduce the values along with the disk loading for the observed data enough to converge the predicted and observed, the disk loading is plotted with the non-dimensional radius in Figure 41. The $R^2$ values do not change, however the values are

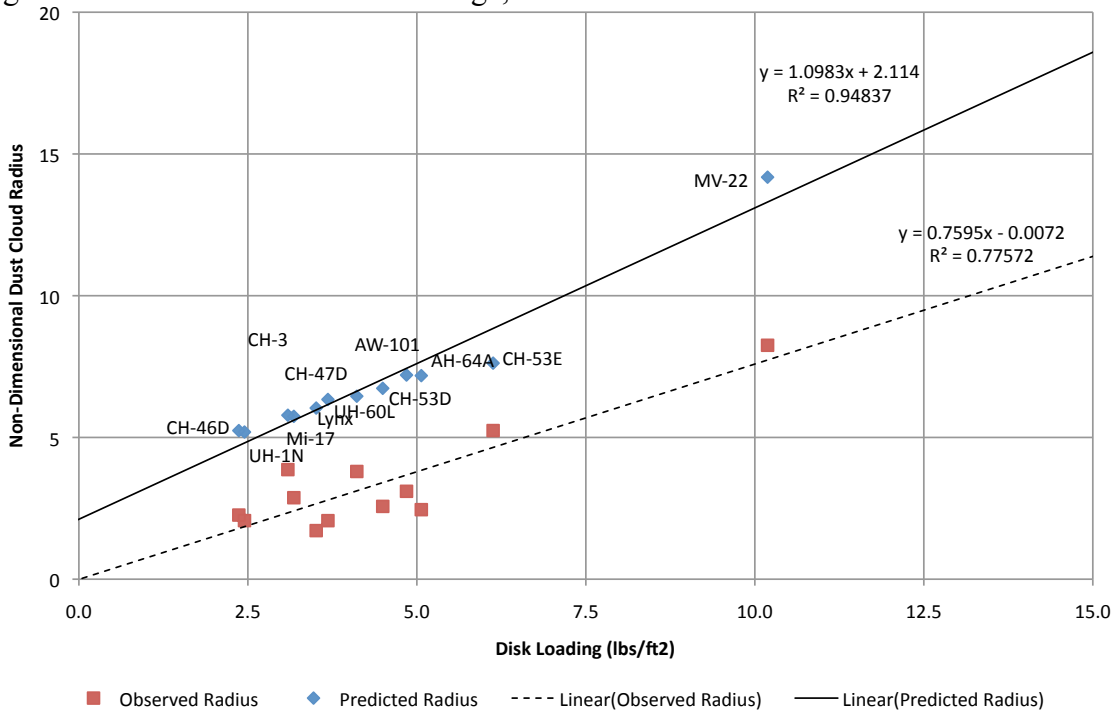


**Figure 41: Approach Power Non-Dimensional Dust Cloud Radius vs. Disk Loading**

much closer. Instead of the observed being roughly 25% to 50% of the predicted as shown in Figure 18, the observed data are 50% to 80% of the predicted values. Even with the adjusted thrust and disk loading values, the predicted values are based on a no wind condition and a fully developed hover. The majority of the test conditions are neither and so the observed data still are expected to be below the prediction, as is the case.

# V. Conclusions and Recommendations

## Conclusions of Research

To this point in rotorcraft design, safety and tactical considerations of operational conditions conducive to DVE have not been taken into account by designers due to insufficient data and predictive design tools. Several means of reducing the dust cloud created by rotorcraft operations in dusty environments exist. These methods are divided among three primary areas; surface treatments, operational procedures, and design criteria. Surface treatments have been examined extensively in previous studies, but have been shelved principally due to the difficulties involved in implementation. Operational procedures are in use with no quantitative way to validate optimum maneuvers. Design criteria have had little prior examination due to limited design tool availability.

From an operational perspective, this work corroborates the practical results in the field and also, in the absence of capable predictive tools, operational procedures have been developed by units that regularly operate in conditions likely to cause dust clouds. These procedures are based on experience, but the successful procedures developed in the field correlate with observations included in this report. Typically, these mitigation procedures include conducting a fast approach (time) at as low a power setting as possible, and landing with as much forward speed as the terrain permits. When the pilot conducts the approach with a low power settings, the descent rate increase, which reduces the time that the rotorcraft can encounter dust that can affect the pilots' perceptions. An approach executed more quickly reduces the time that the dust cloud is allowed to

develop, which will reduce the dust cloud size. A setting a low power condition is also important because it reduces the effective the disk loading on the rotor system, demonstrated to be one of the most important factors in determining the size of the dust cloud. The pilot rating scale presented in this report can augment the existing procedures in use operationally by giving pilots a precise evaluative tool.

From a rotorcraft design standpoint, more work is needed, but the analysis gives results for most modern rotorcraft that could be applied in future designs. For design criteria, the primary driver of the characteristics of the dust cloud produced by rotorcraft is the disk loading. This is true in the absolute sense, but is even more apparent when the dust cloud size is non-dimensionalized by the radius of the rotorcraft main rotor. As shown in this and previous analysis as the disk loading of a rotorcraft increases, the size, both in height and radius, of the dust cloud created increases.

However, it is also clear that the height of the rotor above the ground when the rotorcraft is on the ground as well as the ground wake impingement are also clearly related to the parameters of the dust cloud produced by the rotorcraft. Additional analysis will be needed to determine the relationship of the main rotor height to the dust cloud characteristics. As the impingement of vortexes on the ground increase, so does the size of the dust cloud. Further investigation is required to determine if that is a causal relationship, or just relates back to design decisions made as disc loading increases.

This analysis also indicates that the ROTWASH program is an accurate upper bound for the dust clouds created by rotorcraft. The relationships between the design factors and the dust cloud are closely related to the observed data. A fully developed hover in a dusty environment with no wind will produce a cloud within 15% to that

which is predicted by the ROTWASH program. If additional data can be gathered, a correction factor could be determined and then applied to the ROTWASH predictions to output a more accurate prediction of operational dust cloud size.

**Recommendations for Implementation of Results**

The data developed in this study shows that the non-dimensional dust cloud radius and height are directly related to the disk loading. This indicates that there is little chance to affect the outcome of rotorcraft brownout characteristics once initial aircraft characteristics are determined. However, there are at least two ways in which the results presented here can be used. First, designers should pay close attention to the disk loading as a parameter that will affect aircraft performance and safety. The designers can utilize the data and ratings to aid in reducing risk when mission requirements involve taking the rotorcraft into DVE conditions. Second, observation of cockpit camera views indicate that there are some intangible aspects of the brownout cloud that are not able to be analyzed without much more advanced measurements, but that can be considered at least qualitatively. To this end, the scale was developed to allow pilots to evaluate specific criteria related to piloting the aircraft in the brownout conditions and turn the qualitative data into quantitative data.

**Pilot Rating Scale**

Utilizing the rating scales developed in this report (Appendix B) augmented by continual collection and processing of additional data using the proposed questionnaire

sheet, data could be collected from multiple testing and operational sites simultaneously. The predictions and aircraft parameters may then be more closely linked to the pilot experiences during specific maneuvers. For example, the average pilot rating for an approach intended to minimize brownout to a designated landing zone (LZ) in various gross weight H-60's at the Yuma Proving Ground could be compared. The same ratings could be used to compare the H-60 to an H-53, V-22, or H-47 at the same LZ during one season to compare both gross weight and configuration effects. As the results of this extensive database are compiled, the predictions and aircraft parameters may then be clearly mapped to the pilot experiences during specific maneuvers. These pilot ratings will actually provide a more mission relatable and therefore more relevant analysis than direct examination of the physical size of the dust cloud parameters.

**Contributions**

The contributions made in this report represent three primary areas, updating of previous research, additional analysis and data development utilizing real world data from current rotorcraft, and development of a method for evaluating a downwash dust cloud from the pilot perspective. These follow-on contributions are complimentary to the FAA's *Rotorwash Analysis Handbook,* which is a cornerstone in the traditional (non-CFD based) understanding of rotorcraft downwash. Three key functions from the original Fortran ROTWASH program are updated for MATLAB in Appendix A. In addition, the observed dust cloud dimensions of a sample of modern rotorcraft are compared to the dimensions predicted by the Handbook and ROTWASH. The

comparison is sufficiently close to corroborate the predictions for the dust cloud for a fully developed hover. Several ways of characterizing the dust cloud, height, radius, and a combination are examined. Ultimately, the most useful method characterization of rotorcraft downwash is reasoned to be from the pilot perspective, and two scales are provided for further research.

**Recommendations for Future Research**

Despite the observations and conclusions that have been made in this report, it is still based on incomplete data, and there is still to be learned. It is recommended that a comprehensive flight test program be conducted with each rotorcraft in the current DOD inventory to evaluate the height, radius, and the optical density of the brownout clouds. Ideally, the testing would also include civilian and coalition rotorcraft as well, to allow for a broader analysis. This extensive test could build a robust database that will allow further validation of the FAA model, and of CFD models and simulator models that have been developed over time. This data will also provide a single database that can be used to predict and understand the differences between the dust cloud parameters that might affect tactical or avionics solutions differently on different rotorcraft. Completing the recommended comprehensive test program would be extremely resource intensive, and the DOD requirement to field near term solutions on existing platforms will likely continue to direct money towards avionics for this retrofit. However, given the high cost in lives and equipment in theater, the expense of becoming proficient in design and operational tactics to minimize brownout would seem a small price to pay.

With current funding limitations and priorities, along with limited range time, as well as aircraft availability, there are substantial issues to overcome. The most practical path forward is to use a simple and low cost way to gather relevant data from a large variety of airframes, pilots, and environments. The avionics brownout solutions currently in work will require extensive testing, but inconsistencies in basic flight experiments and restrictions on use of proprietary data will most likely inhibit the collection, availability, and ultimately the usefulness of the database for brownout research. However, the pilot rating scales developed can be used while testing brownout avionics solutions. The rating scales can also be used to collect data from operators flying in DVE-prone operational environments. This could allow for developing brownout mitigating approach techniques or compiling extensive data on a consistent basis. This could allow further extension of the conclusions of this examination and find out if the pilot perception of the brownout severity agrees with modeling indicated by the size and optical density of the brownout cloud. A future analysis of compiled data could provide a valuable and definitive answer.

## Appendix A: ROTWASH MATLAB functions

```
function [RCR,RVR,ZVR,HCR,RCI,RVI,ZVI,HCI,QSMX] =
pcloud(RN,YSP,R,GW,DN,HAGL,SIGPR,XKT,SHFTAN)
%pcloud Summary of this function goes here
%   Detailed explanation goes here

%   Set constant

RHOSL = .0023769 ;
DRC = pi/180 ;

%   Adjust Geometry id Shaft Angle > 0.0 degrees

RSHFT = SHFTAN*DRC ;
CSHFTA = cos(RSHFT) ;
DXO = HAGL*tan(RSHFT) ;

%   Non Dimensionalize Some Parameters

H = HAGL / R / CSHFTA ;
YSEP = YSP / 2.0 / R ;
EFFGW = GW*(1.0 + (DN / 100.00)) ;
DL = EFFGW / RN / pi / R^2 ;
RHO = SIGPR * RHOSL ;
RHOD2 = 0.5 * RHO ;

%   Accelerated Slipstream Mean Velocity

UN = sqrt(2.0*DL/RHO) ;


%   Ground Effect Correction

AKG = 1.0 - 0.9 * exp(-2.0*H) ;


%   Mean Velocity at Rotor Disk (Ratio to UN)

UB = AKG/2.0 ;
```

```
%   Find Initial Radius of wall jet

[ RJ, QSMAX, UN, UMB, UMJ, ZMJ, ZBJ, CU] = waljet( H, UB,
UN) ;


%   Find Cloud Dimensions

[RCR,RVR,ZVR,HCR,RCI,RVI,ZVI,HCI] =
cloud(XKT,UN,UMB,CU,RHOD2,YSEP,R);

%   QS Max

QSMX = RHOD2 * ((sqrt(QSMAX)*UN)^2) ;

end

function [RCR,RVR,ZVR,HCR,RCI,RVI,ZVI,HCI] =
cloud(XKT,UN,UMB,CU,RHOD2,YSEP,R)
%cloud Summary of this function goes here
%   Detailed explanation goes here

XKT = sqrt(XKT) ;
ERC = -0.437 ;
XUM = (UMB*UN)^2 ;
XCU = CU*CU ;

C1 = 1.0 ;
C2 = 2.2 ;

%   Single Rotor Cloud Boundary Calculations

RCR = R*((XKT/(C1*RHOD2*XUM*XCU))^ERC) ;
RVR = 0.785*RCR ;
ZVR = 0.329*RCR ;
RCVR = RCR - RVR ;
AR = (2.0/pi)*log(ZVR/RCVR) ;
PHIR = (pi/2.0)*log(RCVR)/log(ZVR/RCVR) ;
AXLV = AR*((-pi/2.0)+ PHIR) ;
XLV = exp(AXLV) ;
HCR = XLV + ZVR ;

%   Interaction Plane Boundary Calculations

    if YSEP >= 0.1

        RCI = R*((XKT/(C2*RHOD2*XUM*XCU))^ERC) ;
```

```
        RVI = 0.785*RCI ;
        ZVI = 0.329*RCI ;
        RCVR = RCI - RVI ;
        AR = (2.0/pi)*log(ZVI/RCVR) ;
        PHIR = (pi/2.0)*log(RCVR)/log(ZVI/RCVR) ;
        AXLV = AR*((-pi/2.0)+ PHIR) ;
        XLV = exp(AXLV) ;
        HCI = XLV + ZVI ;

    else
        RCI = RCR ;
        RVI = RVR ;
        ZVI = ZVR ;
        HCI = HCR ;
    end
end
```

```
function [ RJ, QSMAX, UN, UMB, UMJ, ZMJ, ZBJ, CU] = waljet(
H, UB, UN)
%waljet Summary of this function goes here
%   Detailed explanation goes here

%   Set Exponents As determined in NASA Manual
EXU = -0.1 ;
EXY = 1.0 ;
EXM = 1.0 + EXU + EXY ;
CZM = 0.28 ;
CZB = 2.8 ;

%   Iterate to find Initial Radius of wall jet

TOL = 1.0E-05 ;
RJ = 2.0 ;

    for I=1,20 ;

        %   Calculation of Equivalent Jet Length

        TR = H + (RJ - 1.0) ;
        TDE = 0.707 * TR ;
```

```
        if TDE <= 3.5
            QSMAX = 1.08 - 0.025 * TDE ^ 2 ;
        elseif TDE > 3.5
            QSMAX = 2.7 / TDE ;
        end

        UM = sqrt(QSMAX) ;
        RJNEW = 2.5 * (UB/UM)^(0.5) ;

        if abs(RJNEW - RJ) <= TOL
            return

        else
            RJ = RJNEW ;
        end

    end

    RJ = RJNEW ;
    UMB = ((0.36*RJ^EXM*(UM*UN)*(UB*UN)^(0.14))^(0.88))/UN
;
    ZHJ = 0.65/(UM/UMB)^2/RJ ;
    CU = UM/UMB*RJ^(-EXU) ;
    CY = ZHJ*RJ^(-EXY) ;
    UMJ = CU*RJ^(EXU)*UMB ;
    ZHJ = CY*RJ^(EXY) ;
    ZMJ = CZM*ZHJ ;
    ZBJ = CZB*ZHJ ;


end
```

## Appendix B: Brownout Rating and Visual Cue Scales

**Data Collection Sheet**

Type/Model/Series_____

Unique Aircraft Configuration _____

Gross Weight for Maneuver _____ Outside Air Temperature _____

Landing Site (LZ)_____ Pressure Altitude of LZ _____

Maneuver Description_____

Approach or profile of interaction with ground_____

Landing Zone Material and Conditions_____

Left Seat Pilot Rating _____ Right Seat Pilot Rating_____

## Pilot Brownout Rating Scale

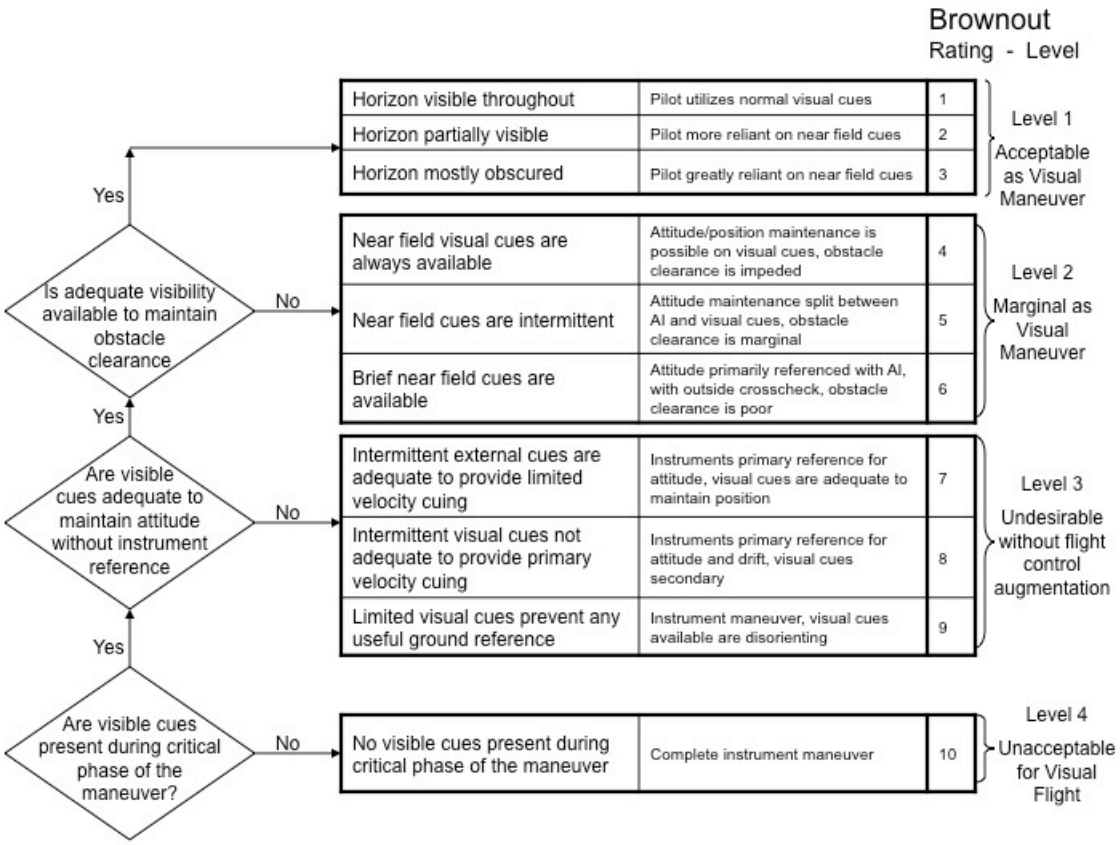


Guide for rating Cues

| Near Field Cue Restriction | Horizon Cue Restriction Due to DVE |
|---|---|
| 0 - no obstruction of near field cues | 0 - no obstruction of horizon |
| 1 - minor/intermittent obstruction of near field cues | 1 - minor/intermittent obstruction of horizon cues |
| 2 - half of near field cues available | 2 - half of horizon cues available |
| 3 - near field cues severely limited by dust | 3 - horizon cues severely limited by dust |
| 4 - dust completely obstructs near field cues | 4 - dust completely obstructs horizon |

NOTE: Suggested control methods for Cue Environments based off ADS-33 spec

| | |
|---|---|
| Level 1 | Rate Control |
| Level 2 | Attitude Command/Attitude Hold |
| | Yaw Rate Command |
| | Heading Hold |
| | Vertical Rate Control |
| | Altitude Hold |
| Level 3 | Three Cue Flight Director |

## Bibliography


Central Intelligence Agency. *The World Factbook 2011.* Washington DC: Central Intelligence Agency, 2011.

Cormier, R. V. *Extremes of Low Atmospheric Density Near the Ground for Elevation up to 15,000 Feet for MIL-STS-201B.* Bedford MA: Air Force Cambridge Research Laboratories, 6 December 1972 (AD0755791).

Cornell Aeronautical Laboratory Inc. *Study of the VTOL Downwash Impingement Problem.* Fort Eustis VA: U.S. Army Transportation Research Command, 1 December 1960 (AD0251154).

Cornell Aeronautical Laboratory Inc. *Theoretical and Experimental Studies of Impinging Uniform Jets.* Fort Eustis VA: U. S. Army Transportation Research Command, April 1963 (AD0408669).

DYNASCIENCES Corporation. *Downwash Impingement Design Criteria for VTOL Aircraft.* Fort Eustis VA: U. S. Army Transportation Research Command, August 1964 (AD0608185).

Ferguson, S. W. *Rotorwash Analysis Handbook, Volume I: Development and Analysis.* Washington DC: Federal Aviation Administration, June 1994 (ADA283719).

Ferguson, S. W. *Rotorwash Analysis Handbook, Volume II: Appendixes.* Washington DC: Federal Aviation Administration, June 1994 (ADA284093).

Franklin, D. and J. Burroughs. *Climate of Iraq*. National Climatic Data Center. 26 May 2009. 26 September 2011. http://www.ncdc.noaa.gov/oa/climate/afghan/iraq-narrative.html.

George, M., E. Kisielowski, and D. S. Douglas. *Investigation of the Downwash Environment Generated by V/STOL Aircraft Operating in Ground Effect.* Fort Eustis VA: U. S. Army Aviation Material Labratories, July 1968 (AD0674644).

Hiller Aircraft Corp. *VTOL Downwash Impingement Study Summary Report.* Fort Eustis VA: U. S. Army Transportation Research Command, August 1961 (AD0264226).

Jackson, P., K. Munson, and L. Peacock. *Jane's All the World's Aircraft 2009-2010*. Jane's Information Group, 2009.

Kuhn, R. E. *An Investigation to Determine Conditions Under Which Downwash From VTOL Aircraft Will Start Surface Erosion from Various Types of Terrain.* Washington DC: National Aeronautics and Space Administration, 1959.

Leishman, J. G. MURI Kick-Off Meeting "Rotorcraft Brownout: Advanced Understanding, Control, and Mitigation". College Park MD, United States, 6 March 2009.

Leishman, J. G. *Principals of Helicopter Aerodynamics.* Cambridge NY: Cambridge University Press, 2006.

McCue, J. *Pitot-Static Systems.* Patuxent River MD: U.S. Naval Test Pilot School, October 1994.

Rodgers, S. J. *Evaluation of the Dust Cloud Generated by Helicopter Rotor Downwash.* Fort Eustis VA: U. S. Army Aviation Materiel Laboratories, March 1968 (AD0669676).

Segall, R. L. *Helicopter Brownout Research.* NASA Ames Research Center. 22 January 2012.
http://rotorcraft.arc.nasa.gov/Research/Programs/brownout.html.

Sissenwine, N. and R. V. Cormier. *Synopsis of Background Material for MIL-STD-210B, Climactic Extremes for Military Equipment.* L.G. Hanscom Field MA: Air Force Cambridge Research Laboratories, 24 January 1974 (AD0780508).

Swenson, R. *AFRL develops partial solution to helicopter brownout.* Eglin Air Force Base News. 9 May 2007. 21 January 2012.
http://www.eglin.af.mil/news/story.asp?id=123052402.

U. S. Army Aviation and Missile Command. *Aeronautical Design Standard Performance Specification Handling Qualities Requirements For Military Rotorcraft*, Redstone Arsenal AL: Aviation Engineering Directorate. 21 March, 2000.

Weather Underground. *Yuma Marine Corps Station Season Weather Averages*. Weather Underground.
26 September, 2011.
http://www.wunderground.com/NORMS/DisplayNORMS.asp?AirportCode=KNYL&SafeCityName=Yuma&StateCode=AZ&Units=none&IATA=NYL.

# REPORT DOCUMENTATION PAGE

*Form Approved*
*OMB No. 0704–0188*

The public reporting burden for this collection of information is estimated to average 1 hour per response, including the time for reviewing instructions, searching existing data sources, gathering and maintaining the data needed, and completing and reviewing the collection of information. Send comments regarding this burden estimate or any other aspect of this collection of information, including suggestions for reducing this burden to Department of Defense, Washington Headquarters Services, Directorate for Information Operations and Reports (0704–0188), 1215 Jefferson Davis Highway, Suite 1204, Arlington, VA 22202–4302. Respondents should be aware that notwithstanding any other provision of law, no person shall be subject to any penalty for failing to comply with a collection of information if it does not display a currently valid OMB control number. PLEASE DO NOT RETURN YOUR FORM TO THE ABOVE ADDRESS.

| 1. REPORT DATE (DD–MM–YYYY) | 2. REPORT TYPE | 3. DATES COVERED *(From — To)* |
|---|---|---|
| 10-09-2012 | Master's Thesis | August 2009 – September 2012 |

**4. TITLE AND SUBTITLE**
Characteristics, Causes, and Evaluation of Helicopter Particulate Obstruction

5a. CONTRACT NUMBER
5b. GRANT NUMBER
5c. PROGRAM ELEMENT NUMBER

**6. AUTHOR(S)**
Sullivan, Michael P., Lieutenant Commander, USN

5d. PROJECT NUMBER
5e. TASK NUMBER
5f. WORK UNIT NUMBER

**7. PERFORMING ORGANIZATION NAME(S) AND ADDRESS(ES)**
Air Force Institute of Technology
Graduate School of Engineering and Management (AFIT/ENY)
2950 Hobson Way
WPAFB OH 45433-7765

**8. PERFORMING ORGANIZATION REPORT NUMBER**
AFIT/GAE/ENY/12-S46

**9. SPONSORING / MONITORING AGENCY NAME(S) AND ADDRESS(ES)**
Intentionally Left Blank

10. SPONSOR/MONITOR'S ACRONYM(S)
11. SPONSOR/MONITOR'S REPORT NUMBER(S)

**12. DISTRIBUTION / AVAILABILITY STATEMENT**
APPROVED FOR PUBLIC RELEASE; DISTRIBUTION UNLIMITED

**13. SUPPLEMENTARY NOTES** This material is declared a work of the U.S. Government and is not subject to copyright protection in the United States.

**14. ABSTRACT**

A comprehensive approach to evaluation of rotorcraft brownout under degraded visual environmental conditions is presented. The results of a literature search covering the current state of brownout research are summarized. The brownout dust cloud generated by modern rotorcraft is analyzed and characterized using photographic and video data, coupled with examination of previous computer modeling techniques. A modeling analysis is performed in order to relate aircraft design and operating parameters to brownout dust cloud size is performed. The effect of vorticity in brownout dust cloud rollup is included. An augmented rating scale for pilot assessment is proposed for operational use, and the results are presented for designers and operators to approximate brownout performance of existing and future rotorcraft.

**15. SUBJECT TERMS**
Helicopters, Rotorcraft, Helicopter Design, Rotor Downwash, Brownout, Ground Effects (Aerodynamic) Pilot Rating Scale, Brownout Parameter

| 16. SECURITY CLASSIFICATION OF: | | | 17. LIMITATION OF ABSTRACT | 18. NUMBER OF PAGES | 19a. NAME OF RESPONSIBLE PERSON |
|---|---|---|---|---|---|
| a. REPORT | b. ABSTRACT | c. THIS PAGE | UU | 113 | Dr. Donald L. Kunz |
| U | U | U | | | 19b. TELEPHONE NUMBER (Include Area Code) (937)255-3636, ext 4548 |

**Standard Form 298 (Rev. 8–98)**
***Prescribed by ANSI Std. Z39.18***